UAV APPLICATIONS IN ROAD MONITORING FOR MAINTENANCE PURPOSES

A DISSERTATION

Submitted to

ASSAM DON BOSCO UNIVERSITY

By

BADABIANGMON DKHAR

Roll No. DC2015MTC0002

in partial fulfilment for the award of the degree

of

MASTER OF TECHNOLOGY

in

CONSTRUCTION ENGINEERING AND MANAGEMENT

DEPARTMENT OF CIVIL ENGINEERING

SCHOOL OF TECHNOLOGY
ASSAM DON BOSCO UNIVERSITY
AZARA, GUWAHATI 781 017,
ASSAM, INDIA.

MAY 2017

UAV APPLICATIONS IN ROAD MONITORING FOR MAINTENANCE PURPOSES

A DISSERTATION

Submitted to

ASSAM DON BOSCO UNIVERSITY

By

BADABIANGMON DKHAR

Roll No. DC2015MTC0002

in partial fulfilment for the award of the degree

of

MASTER OF TECHNOLOGY

in

CONSTRUCTION ENGINEERING AND MANAGEMENT

DEPARTMENT OF CIVIL ENGINEERING

SCHOOL OF TECHNOLOGY
ASSAM DON BOSCO UNIVERSITY
AZARA, GUWAHATI 781 017,
ASSAM, INDIA.

MAY 2017

CERTIFICATE

This is to certify that the Dissertation entitled "**UAV APPLICATIONS IN ROAD MONITORING FOR MAINTENANCE PURPOSES**" submitted by **BADABIANGMON DKHAR (Roll. No. DC2015MTC0002)** to the Assam Don Bosco University, Guwahati, Assam, in partial fulfilment of the requirement for the award of degree of **Master of Technology in "Construction Engineering and Management", Department of Civil Engineering,** is a bona-fide record and the project work carried out by **her** under my supervision during the year **2016-2017** is satisfactory.

(N.Thoiba Singh),
Assistant Professor,
Department of Civil Engineering,
School of Technology,
Assam Don Bosco University

Dated 2017

Place: Guwahati

CERTIFICATE

This is to certify that the Dissertation entitled "**UAV APPLICATIONS IN ROAD MONITORING FOR MAINTENANCE PURPOSES**" submitted by **BADABIANGMON DKHAR (Roll.No.DC2015MTC0002)** to the Assam Don Bosco University, Guwahati, Assam, in partial fulfilment of the requirement for the award of degree of Master of Technology in Construction Engineering and Management, Department of Civil Engineering, is a bona-fide record and she successfully completed the project work during the year 2016-2017.

(Dr. Girija T. R),
Associate Professor and Head,
Department of Civil Engineering,
School of Technology,
Assam Don Bosco University

Dated 2017

Place: Guwahati

(Dr. Manoranjan Kalita),
Director
School of Technology,
Assam Don Bosco University

Dated 2017

Place: Guwahati

DECLARATION

I hereby declare that the Dissertation work entitled "**UAV APPLICATIONS IN ROAD MONITORING FOR MAINTENANCE PURPOSES**" submitted to the Assam Don Bosco University, Guwahati, Assam, in partial fulfilment of the requirement for the award of degree of Master of Technology in Construction Engineering and Management, Department of Civil Engineering, is an original work done by me under the guidance of Shri. Chirag Gupta and Shri. N. Thoiba Singh, and has not been submitted for the award of any degree.

(Signature of the student)

BADABIANGMON DKHAR

DC2015MTC0002

Civil Engineering department

Dated 2017

Place: Guwahati

ACKNOWLEDGEMENT

I would take this opportunity to thank each and everyone who has helped me in my M.Tech project. Firstly, I would like to express my gratitude to Shri. Chirag Gupta, Scientist/Engineer 'SC', NESAC for guiding me with the best knowledge and helping me to finish my project work in time and a successful one.

I would also like to express my deepest gratitude to the director of North Eastern Space Applications Centre (NESAC), Umiam, Meghalaya, Shri. P.L.N Raju, for believing in me and allowed me to work under his organization and for providing me with the necessary facilities and resources needed for my project work.

I would especially like to thank Shri. N.Thoiba Singh, Assistant Professor, Department of Civil Engineering, Assam Don Bosco University, who has helped me to complete my project satisfactorily and according to the required standard.

I would also like to express my sincere thanks to Dr. Girija T R, Associate Professor and Head, Department Of Civil Engineering, School of Technology, Dr. Manoranjan Kalita, Director, School of Technology and to all the faculty of Department of Civil Engineering, Assam Don Bosco University for their words of encouragement.

Lastly, I would like to thank my family and friends who supported me throughout the project work.

ABSTRACT

Maintenance is important for roads in order to improve the design life. Without proper maintenance, deterioration of roads will occur more rapidly which will later incur loss in both time and cost. For maintenance of roads, proper condition survey needs to be done before taking up the repair work and cost estimation. Usually, the condition survey is done by vehicle or on foot, which is time consuming, more number of people and more expenditure involved. In the end, the roads do not get surveyed and maintenance work is hence delayed. This becomes a problem to the public as well as the government. In order to improve the road monitoring system for maintenance purposes, Unmanned Aerial Vehicle (UAV) is proposed and used in portion of the roads in Bhoirymbong, Sumer 4 No and Umtham which are under Umsning C and RD Block, Ri Bhoi District of Meghalaya, India. The implementation and results shows that an emerging technology like UAV, can be used for maintenance purposes because of its many advantages like its real time monitoring capabilities, flexibility and ease of manoeuvrability, etc. and it will give a time saving and cost effective solution. The method performance of the test images processed in MATLAB software resulted in overall Precision of 96.57%, Recall of 75.80% and Tracking Accuracy of 74.13%.

KEYWORDS: *Maintenance, Condition Survey, Road Monitoring, Unmanned Aerial Vehicle (UAV).*

CONTENTS

LIST OF TABLES

LIST OF FIGURES

ABBREVIATIONS

UAV	Unmanned Aerial Vehicle
RUAV	Rotorcraft Unmanned Aerial Vehicle
VTOL	Vertical Take-Off and Landing
GPS	Global Positioning System
NRRDA	National Rural Road Development Agency
WBM	Water Bound Maccadam
MAV	Micro Air Vehicle
GUI	Graphic User Interface
RGB	Red Green Blue
ODR	Other District Road
ROI	Region of Interest
TP	True Positive
FP	False Positive
TN	True Negative
FN	False Negative
GCP	Ground Control Point
CAD	Computer Aided Design
DSM	Digital Surface Model
wd	Working day

CHAPTER 1

INTRODUCTION

1.1. INTRODUCTION TO UAV

UAVs are designed and assembled based on the requirements and are mainly classified into two categories: i) **Fixed-wing** and ii) **Rotorcraft** or **Multirotor** or **Rotary wing UAVs**. Fixed-wing UAVs have limitations in terms of complex designs, difficult stabilizing mechanism, requirement of a long runway and difficult to operate in hilly terrain. However, they have advantages in terms of long endurance and large payload capabilities. Multirotor UAVs use Vertical Take-Off and Landing (VTOL) and are found more appropriate in hilly or complex terrain. Fixed Wing UAVs has been around since World War II primarily to be used as target dummies during training. These types of UAVs are fast, expensive and can operate for several hours, hence, have been predominantly used in the military, whereas, the Rotorcraft/Multirotor UAVs are cheaper, slower and cannot operate for long. The RUAVs hence is predominantly used by individuals and companies.

In the past 10 years many small quadcopters have entered the markets that include the DJI Phantom and Parrot AR Drone. This new breed of quadcopters is cheap and lightweight. In the 20th Century, military research precipitated many widely used technological innovations. Surveillance satellites enabled the GPS-system and defense researchers developed the information swapping protocols that are fundamental to the Internet. Drones fall into a similar category. Designed initially for reconnaissance purposes, their para-military and commercial development was often out of sight of the public.

Rotary Wing or Rotorcraft UAV is an aircraft which relies on a rotor to move which in turn generates lift, allowing the aircraft to fly. An example of a rotary wing aircraft is the Helicopter. In case of a rotary wing aircraft, the wings connected to the rotor mast moves. This rotating movement of the propellers/rotors generates the necessary velocity over the airfoil to generate lift. Since the velocity over the wings is being generated by moving the rotors, RUAVs are capable of VTOL and thus can be used in areas where there is lack of space or where focus on a certain area is required for an extended period of time. The

presence of the rotary wing model also ensures very high maneuverability and the ability to hover in a set point in space for a long time. However, unlike most fixed wing models of UAVs, the rotary wing models generally have a much shorter flight time. Most rotary wing based UAVs are multirotor, with generally more than one rotor. The rotary wing UAVs can be further divided based on the number of motors used and the configuration the motors are set up in.

The North Eastern region of India is located in the foothills of the Himalayas and hence lies on the boundary of the Indian and the Eurasian tectonic plates. To map and survey such a region requires frequent updates to the existing maps as the topography of the region frequently changes. The frequent updating of the map can be done in two ways, through a camera flying in the sky or a camera flying in space.

The merits of using UAV in monitoring purposes includes:-

i) UAVs can be programmed offline and controlled in real time to navigate and to collect data using a variety of multiple and interchangeable imaging devices and other sensors.
ii) UAVs can be flown at a lower altitude, has more flexibility and maneuverability and can collection high resolution data which can give detailed images and models.
iii) The UAVs with respect to particular applications has more advantage than satellite imagery like detailed survey of an area, to generate the Orthomosaic image.
iv) It aids in monitoring urgently in natural disaster like earthquakes, floods, landslides, etc.
v) UAVs are becoming easier to use, more durable and reliable and are increasingly marketed to those with little experience or training. Their cost is diminishing, while technical capabilities improve.

The UAV is expected to be light, small, portable, and reliable, and should be able to access regions and areas which would otherwise not be accessible on foot or any other mode of transport other than flight. This UAV is then required to take high quality images, which is to be geo-tagged, and then sent to the remote sensing team in the lab for analysis.

1.2. ROAD MAINTENANCE

As per NRRDA Guidelines, the Indian Roads Congress defines road maintenance as "Routine work performed to upkeep pavement, shoulders and other facilities provided for road users, as nearly as possible in their constructed conditions under normal conditions of traffic and forces of nature".

1.2.1. Types of road maintenance

There are three types of road maintenance operations which include: -i) Routine, ii) Periodic and iii) Emergency maintenance.

i) **Routine Maintenance:** This kind of maintenance is scheduled to be done at fixed times during the year as specified by the department concerned and is required to do on every road regardless of its engineering characteristics or its traffic volume. The works under this maintenance is usually small scale, for example, repairing of potholes, patches, etc. and requires manual labour and does not incur much cost.

ii) **Periodic maintenance:** This is carried out in addition to the routine maintenance and involves more comprehensive and costly activities such as reshaping of the road surface, re-surfacing and major repair or reconstruction of cross-drainage structures and requires more equipment and specialist skills. The periodic maintenance works would be scheduled at intervals of 3 to 7 years, depending on traffic levels, pavement type, geographical and weather conditions, quality of the road and the level of wear and tear.

iii) **Emergency Maintenance** responds to occasional, unforeseen events such as erosion, landslides, large trees or debris on the road and broken drainage structures. Emergency maintenance can be categorized into:

(a) Temporary restoration works, re-opening safe passage on the road, and

(b) Permanent restoration, securing the stability of the road and reinstating all its components to its former (or a better) condition.

1.3. ROAD CONDITION SURVEY

Road maintenance is an important operation to be done so that the roads can have a longer life and prevent it from long term deterioration due to the pavement defects. Road maintenance requires careful planning, supervision and monitoring. Before planning and implementation of the work, a detailed survey of the existing road condition during which all defects and damages to the road are carefully assessed so that the proper estimate will be done for the maintenance work.

In order to assess the needs for and to plan future improvement and road maintenance works, it is necessary to maintain up-to-date information about the condition of the road network and hence, it is a good practice to carry out regular road condition surveys. Such surveys form a solid basis for future work planning and budgeting. Road condition surveys allow the road authority as follows:

i) to become thoroughly familiar with the road network and its maintenance challenges and on this basis, make objective and quantified assessments of the condition of each road,
ii) to make objective prioritizations of maintenance and improvement works in line with sound asset management principles,
iii) to review the effectiveness of maintenance activities carried out since the previous surveys, and
iv) to program the improvement and maintenance works to be carried out during the next construction season.

Usually, these inspection works are carried out manually on foot or vehicle. The inspector also has to take safety measures like wearing reflective clothing for safety from passing vehicles at all times. This kind of inspection usually takes time and the wage payment for the inspector is depended on the task rate per working day. In India, the road network is vast and every state is mainly connected by roads. Due to the size of the road network, surveys carried out to monitor its condition are time consuming and costly. In a country like India, the funding also becomes a problem due to insufficient allocation of funds by the government and also ineffective use of available funding due to the lack of proper data and information about the conditions of the roads. As the road network is large and official

staffs are less, sometimes, the road network does not get surveyed and hence, monitoring the condition of roads becomes a problem.

1.4. PAVEMENT DISTRESS

Pavement distress is any type of pavement defect which will indicate a decline in the pavement's surface condition or structural load carrying capacity. This will result in the poor or unsatisfactory performance of the pavement due to its impending failure.

1.4.1. Types of pavement defects

i) Ruts are caused by the deformations in pavements with insufficient strength to cater for the prevailing traffic, mostly as a result of improper mix design, weak pavement, intrusion of sub-grade clay into base course, poor compaction works or overloaded vehicles. It often takes place on roads with a high prevalence of heavy traffic for which the pavement was not designed. Un-drained water penetrating the surface can further weaken the pavement leading to more deformations and finally breaking the surface.

Figure 1: Rutting. (Source: NRRDA Guidelines, 2014)

ii) Potholes are depressions that occur on sections of the road where the road base has been exposed to high moisture levels due to cracks on the paved layer. The causes can be due to lack of proper bond between the bituminous surfacing and underlying WBM, insufficient bitumen content and too thinly laid bituminous wearing course. Potholes are a common surface defect on both paved and unpaved roads. They develop under the action

of tyres, especially from heavy vehicles. For roads with a sound base course, they eventually develop when the surface seal is worn out. Potholes increase rapidly in size during the rainy season when water collects inside the hole and often develop as a result of poor drainage of the base course.

Figure 2: Pothole. (Source: Pavement Interactive)

iii) Edge failures of paved roads are caused by weak materials used in shoulders and poor shoulder maintenance that leaves the surface of the road pavement higher than the adjacent shoulder. Edges are often more vulnerable to settlements due to shoulders consisting of poor materials or with poor drainage.

Figure 3: Edge failure. (Source: NRRDA Guidelines, 2014)

iv) Ravelling is a process in which the surface layer loses its aggregate particles due to insufficient binder in the surface seal. This may take place when there is insufficient bonding with the underlying surface or from an uneven application of binder when applying a chip and spray seal. Equally, incorrect binder content in a surface premix may cause ravelling. Ravelling can take place if the surface seal is poorly spread and compacted, construction during wet weather, excessively open graded mix and overheating of the binder or aggregate.

Figure 4: Ravelling. (Source: NRRDA Guidelines, 2014)

v) Delamination is a result of poor bonding with the underlying surface or insufficient stability of the wearing course, resulting in a total loss of the surface seal. The loss of the surface seal may eventually lead to the development of potholes unless the defect is addressed by patching or resealing the failed section.

Figure 5: Delamination. (Source: NRRDA Guidelines, 2014)

vi) Cracks in the road surface can develop in various patterns and frequency. Most cracks are caused by movements or settlements in the underlying pavement layers as a result of poor materials or workmanship, instability of fills and shoulders or movements in the sub-grade. If left unattended, cracks develop into potholes, causing further damage to the pavement and its surface. The frequency of cracks provides some indication of which layer of the pavement is causing the settlement. When there are less frequent cracks, the settlements are likely to originate from the deepest layers in the pavement, i.e. the sub grade or sub-base.

Figure 6: Cracks. (Source: Emaze)

vii) Depressions are caused by the uneven settlement of the pavement layers. Depressions are more common on older roads with limited pavement strengths and which is experiencing an increase in heavy traffic. Depressions on new roads are either a result of construction faults, using poor quality materials or when the drainage fails resulting in the pavement being saturated with water. Depressions can also develop as a result of differential movements at structures, often found at bridge and culvert approaches.

Figure 7: Depression. (Source: LGAM)

viii) Bleeding is a result of excessive amounts of bitumen binder in the surface seal which forces the road surface by the action of traffic. The spot where bleeding has occurred is soft and has a smooth surface and reduces skid resistance, especially when wet. In extreme cases, the surface layer may separate and break away under the action of traffic.

Figure 8: Bleeding. (Source: E-Sun Heavy)

ix) Corrugations are transverse wave patterns occurring on carriageway formed mainly during the dry season on gravel or earth roads on which high proportions of loose material exists. As the traffic passes, the loose material is pushed into regular lumps across the road forming deeper corrugations.

Figure 9: Corrugation. (Source: Pan Sci)

x) **Shoving** is the formation of ripples across a pavement. This characteristic shape is why this type of distress is sometimes called wash-boarding. Shoving occurs at locations having severe horizontal stresses, such as intersections. It is typically caused by: excess asphalt; too much fine aggregate; rounded aggregate; too soft asphalt; or a weak granular base.

Figure 10: Shoving. (Source: Paveman Pro)

1.5. ROAD INVENTORY DATA

According to the Ministry of Rural Development, Government of India, The data collected from the survey is recorded as Road Inventory Data for every one kilometer (km). Based on this Road Inventory Form, the estimate for cost and budgeting will be done. By the time the actual work of maintenance will take place, there might have been some more pavement distress; hence the estimate should not be so exact keeping in mind that future costs might incur. This kind of planning is not accurate and the cost estimate will either be less or more than the required. Hence, it becomes a problem and many roads remain un-monitored and therefore no maintenance work is done. This results in loss of time as well as loss of money. Due to the shortage of staff also, another inspection is not possible. The format for Road Inventory Data is given in Table 1.

Table 1: Example of a Road Inventory Form.

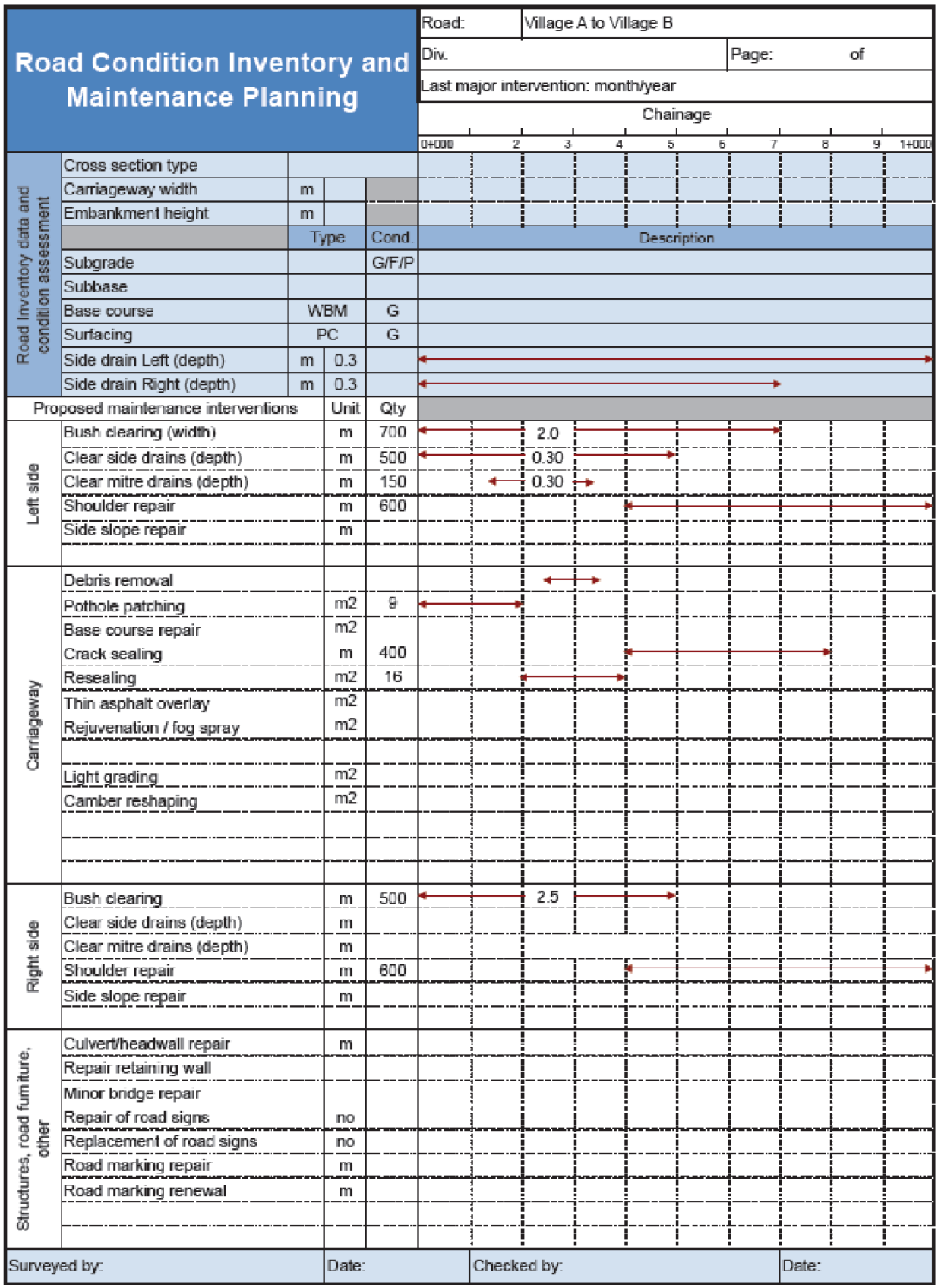

Road Condition Inventory and Maintenance Planning					Road: Village A to Village B									
					Div.					Page: of				
					Last major intervention: month/year									
					Chainage									
					0+000	2	3	4	5	6	7	8	9	1+000
Road inventory data and condition assessment	Cross section type													
	Carriageway width	m												
	Embankment height	m												
		Type		Cond.	Description									
	Subgrade			G/F/P										
	Subbase													
	Base course	WBM		G										
	Surfacing	PC		G										
	Side drain Left (depth)	m	0.3											
	Side drain Right (depth)	m	0.3											
Proposed maintenance interventions			Unit	Qty										
Left side	Bush clearing (width)		m	700		2.0								
	Clear side drains (depth)		m	500		0.30								
	Clear mitre drains (depth)		m	150		0.30								
	Shoulder repair		m	600										
	Side slope repair		m											
Carriageway	Debris removal													
	Pothole patching		m2	9										
	Base course repair		m2											
	Crack sealing		m	400										
	Resealing		m2	16										
	Thin asphalt overlay		m2											
	Rejuvenation / fog spray		m2											
	Light grading		m2											
	Camber reshaping		m2											
Right side	Bush clearing		m	500		2.5								
	Clear side drains (depth)		m											
	Clear mitre drains (depth)		m											
	Shoulder repair		m	600										
	Side slope repair		m											
Structures, road furniture, other	Culvert/headwall repair		m											
	Repair retaining wall													
	Minor bridge repair													
	Repair of road signs		no											
	Replacement of road signs		no											
	Road marking repair		m											
	Road marking renewal		m											
Surveyed by:			Date:		Checked by:					Date:				

(Source: Managing Maintenance of Rural Roads in India, NRRDA, 2014)

In order to solve this lack of information and data, this research work is done with the use of Unmanned Aerial Vehicle (UAV) or drones. The use of UAV proves to be effective and time-saving as well as cost-effective. The data collected is in the form of images. With the use of UAV, the concerned person can go and finish the surveying work in a day and the comparison of the old and new data can be verified accordingly. The maintenance work can also be monitored and the scheduling of activities can be done accordingly and proper decisions and planning can be made.

1.6. OBJECTIVES OF THE RESEARCH

The objectives of the research work are as follows:

i) To acquire the data using UAV in the form of very high resolution images.

ii) Processing of the data using MATLAB software. The outputs generated are-Filled Image/Closed Image and Region of Interest Image (ROI) Image.

iii) Method performance analysis of the data obtained.

iv) An information system can be generated with the use of the ROI image and input in Google Earth to show as a map or path denoting the road distress location according to its priority, i.e., from highest to lowest pavement distress location.

v) In Pix4d software, the pavement distresses can be located by drawing polylines in the point clouds and exported as shape files.

vi) The Orthomosaic generated in Pix4d software and the polylines from the point clouds can also be exported to AutoCAD Civil 3D software to further locate the pavement distress and can be represented as a map.

CHAPTER 2

LITERATURE SURVEY

Zhang (2008) Unmanned Aerial Vehicle (UAV) is used for monitoring the condition of unpaved roads by collecting the data in the form of images. The washboarding effect in unpaved roads can be detected by pattern recognition and image classification techniques in the UAV imagery.

Koch and Brilakis (2011) The collection of data for pavements has been done by vehicles but the time taken to analyze each image or video is done manually and is time consuming. The proposed method is to automate the existing process of pothole detection in visual pavement data. The pavement image is first divided into defect and non-defect regions then shape extraction is done followed by texture comparison. This methodology has been implemented in a MATLAB prototype with an overall Accuracy of 86%, Precision of 82% and Recall of 86%.

Eschmann et al. (2012) A rotary wing octocopter micro air vehicle (MAV) system has been used to scan buildings for inspection and monitoring purpose with a high resolution digital camera. For building inspection the data acquisition (by aerial survey, in-flight) where manual flight control is performed to fly close to the buildings and digital post-processing (post flight) is done. Vertical movement flight pattern of the MAV increased lens-induced effects negative for stitching, hence horizontal movement is preferred and this inspection data acts as the first data base for further planning and maintenance activities.

Jog et al. (2012) In the U.S, roadways are usually maintained by dedicated vehicles that collect pavement surface video and profile data. These data are then evaluated manually by technicians on computers which is a time-consuming task. Therefore, the proposed method involves collection of videos of the roadway which contains potholes. These videos are divided into consecutive frames and through visual 2D recognition the number of potholes can be detected and through 3D reconstruction the width and depth of the pothole can be analyzed automatically in order to assess the severity of the pothole.

Adlinge and Gupta (2013) Before going to the maintenance strategies, it is important to know the types of pavement and accordingly the pavement functions, like, to provide a smooth riding surface, provide adequate surface friction, protect the sub grade and provide waterproofing surface. Throughout the life of the pavement certain factors influence its performance, i.e., traffic, moisture, sub grade, construction quality and maintenance. Due to these factors the pavement may undergo deterioration and its causes should be understood carefully before doing the maintenance work.

Siebert and Teizer (2014) Explain about the use of UAV in earthwork projects. The UAVs and its flight planning software tool are explained in order to know which UAV is best suited for a particular project and the comparison is done with conventional method of surveying to evaluate its performance in test bed and field realistic environments.

Liu et al. (2014) UAV developments shows that it can aid in various applications for civil engineers like in seismic risk assessment, transportation, disaster response, construction management, surveying and mapping and flood monitoring and assessment. However, some challenges also occur, but due to its capacity to do large scale work many new opportunities are available than using the conventional or traditional methods.

Buchinger and Silva (2014) Road conditions should have both quality (comfort and safety) and performance (travel more in less time). However, some anomalies occur which compromises with its good condition and due to the vast network of roads, it becomes a difficult task to monitor the entire road network. Therefore, several road network maintenance programs have been established to assess the road conditions. A new vision based algorithm for road anomalies detection, such as potholes and cracks, using morphological image processing is done by collecting the data by an embedded camera to obtain like Google street view concept and then the road segmentation is done followed by morphological image processing. This algorithm is done on 186 images and resulted in Accuracy- 84%, Precision- 75.68% and Recall- 90.32%.

Radopoulou and Brilakis (2015) Pavement management systems rely on comprehensive up to date road condition data to provide effective decision support for maintenance scheduling. The data is collected for the detection and tracking of patches in video frames

with the use of a vision tracker by utilizing the car parking camera and processing is done by a detection method using image processing techniques. The proposed solution is inexpensive with Precision- 84% and Recall- 96%.

Kim et al. (2015) Unmanned Aerial Vehicle (UAV) will be able to conduct a safety check and inspect high areas and narrow passages which are difficult or impossible to access by manpower to ensure safety of the structure. A crack detection algorithm in order to detect the crack and width of the structure automatically was developed combining applications of UAV and digital image analysis techniques by morphology method and the field test was conducted on bridges.

Sankarasrinivasan et al. (2015) The approach of using UAV for data acquisition is the foundation for a cost effective and time saving solution for monitoring of large civil structures. The image processing is done by MATLAB GUI interface. The image processing and data acquisition procedures are for crack detection and assessment of surface degradation.

Vacanas et al. (2015) Time in infrastructure construction projects is very important. Any delay might incur loss or disputes among the client and contractors. So, UAV have been used to collect visual records and incorporate with Building Information Modeling (BIM) technology in order to know the cause of delays so that further decisions can be taken to help incur less cost and disputes. Comparison was also done with the traditional method of inspection to collect data and disruption analysis.

Costa et al. (2016) Unmanned Aerial Vehicles (UAVs) are used for the safety inspection of a building. The UAV was used for two construction sites in Brazil and the information gathered in real time could provide information and visualization of 87.2% and 58% of the safety inspection items established in Project A and Project B of the two construction sites respectively. There was no damage or interference due to the UAV except stopping the crane for some time. This information can also contribute to decision making process.

CHAPTER 3

METHODOLOGY

3.1. DATA COLLECTION

The collection of data is done with the use of UAV. The UAV used for the research work is a Rotary wing UAV which consist of four motors and is called a Quadcopter which has an RGB camera of 12 Megapixel with an optical sensor and runs on Lithium polymer batteries (Gupta et al., 2016). It can fly up to 500 m altitude and it can be controlled either by autonomous mode or manual mode. The data processed shows that UAV images with its high resolution and geo-tagging properties are able to capture the road defects.

Geo-tagging is the process of adding geographic information to various media in the form of metadata. The data usually consists of coordinates, like latitude and longitude but may even include altitude, bearing, distance and place names.

Figure 11: Rotary wing UAV (Quadcopter).

Table 2: Technical specification of aircraft and the camera of the UAV.

Aircraft		Camera	
Model	DJI Inspire 1 (T600)	Name	X3
Weight(Battery Included)	2935 g	Model	FC350
Dimensions	438x451x301 mm	Effective Pixels	12.4M
Hovering Accuracy (GPS mode)	Vertical: 0.5 m Horizontal: 2.5 m	FOV (Field of View)	94°
Max Speed	22 m/s (ATTI mode, no wind)	Photo/Video format	JPEG, DNG/MP4 MOV
Max range	2000 m radius (with line of sight)	Lens	20mm Anti-distortion
Max Height	2500 m	Still Photography Modes	Single shoot Burst shooting: 3/5/7 frames Time-lapse
Max Wind Speed Resistance	10 m/s	Video Recording Modes	UHD (4K), FHD, HD
Max Flight Time	Approximately 18 minutes (per battery)	Supported SD Card Types	Micro SD Max capacity: 64 GB. Class 10 or UHS-1 rating required.

(Source: Gupta et al., 2016)

3.2. IMAGE PROCESSING

The images collected with the help of the UAV are first processed using MATLAB R2013a software. The images are first enhanced by stretching the original image in order to highlight the color of the elements in the image. The enhanced image is then converted to a gray scale image. Gray-scale values range between 0, which represents black, and 255, which represents white (Radopoulou and Brilakis, 2015). Then the segmentation of the image is done by thresholding in order to convert the gray image into a binary image. This allows the separation of the darker regions of the pavement image, which in most cases

represent the defective areas from the background. The threshold level varies and depends on the image processed. After segmentation, morphological operation is done in order to connect the components of the binary image to get a filled image for defects like potholes and closed image for defects like cracks.

The filled image or closed image is then used to create Region of Interest (ROI) of the pavement distresses or defects. From these ROI, the area of pavement distress is calculated in terms of pixels and the image number which has the maximum number of pixels will be the one with the most severe defects and so on. The severity analysis of the pavement distress can be prioritized accordingly and these data can be used as an information system in maps like Google earth to the Surveyors or Engineers in-charge for them to make decisions, that which segment of the road is to be maintained first and accordingly do the scheduling and cost of the road maintenance work.

In the MATLAB codes, the threshold value will vary for each image. The MATLAB codes used for image processing are given in **Appendix B**.

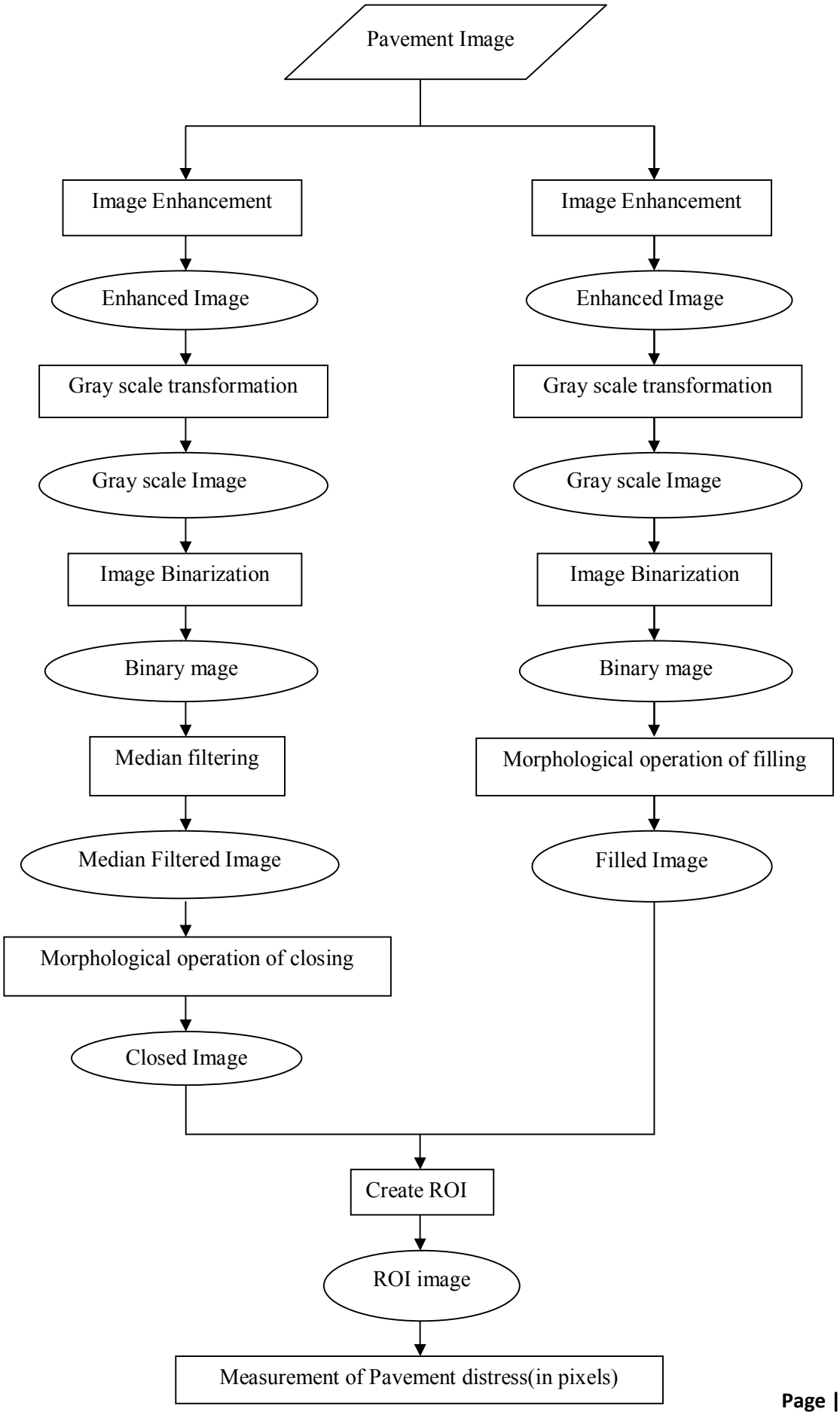

Figure 12: Flowchart for measuring the pavement distress method.

3.3. METHOD PERFORMANCE ANALYSIS

To measure the performance of the proposed method three metrics were used: **Precision, Recall** and **Accuracy**. Precision is related to the detection exactness and is described by Eq. (1); Recall refers to the detection completeness and is defined by Eq. (2); and Accuracy refers to the average correctness of the process and is described by Eq. (3). In the equations TP stands for True Positive (correctly detected), FP stands for False Positive (incorrectly detected), TN stands for True Negative (correctly not detected) and FN stands for False Negative (incorrectly not detected) (Radopoulou and Brilakis., 2015). The processed image (Closed or Filled Image) is manually checked with the original UAV image for TP, FP, TN and FN.

$$\text{Precision} = \frac{TP}{TP+FP} \tag{1}$$

$$\text{Recall} = \frac{TP}{TP+FN} \tag{2}$$

$$\text{Accuracy} = \frac{TP+TN}{TP+FP+TN+FN} \tag{3}$$

3.4. GENERATION OF 3D POINT CLOUDS AND ORTHOMOSAIC

Pix4d Mapper Pro software is for professional drone-based mapping purely from images taken by a drone or UAV. It delivers highly precise geo-referenced 2D maps and 3D models which compliment a wide range of applications and software. Key outputs of Pix4d Mapper Pro are:

i) 3D point cloud
ii) Digital Surface Model
iii) Orthomosaic
iv) Volume calculation
v) Contour lines
vi) 3D textured model

The images taken with the help of UAV are processed with the help of this software in order to generate the Orthomosaic and 3D point clouds**.**

Point cloud: A Point cloud is a set of three-dimensional distributed points usually defined by X, Y and Z coordinates which result from a laser or photogrammetry scan and are often intended to represent the external surface of an object. Each point cloud is calculated by matching several photographs (in the case of photogrammetry survey) so as it corresponds to a point of the surface of the survey object. The density of a point cloud is dependent on the quantity and quality of the photos taken, but also the way the photographs were taken or the angle or projection of capturing the images.

Point cloud files support the design process by providing real world context where the referenced objects can be recreated or additional models can be inserted. Once a point cloud is attached to a drawing, it can be used as a guideline for drawing, change its display, or apply a color stylization to distinguish different features.

Orthomosaic: The Orthomosaic is a 2D map. Each point contains X, Y and color information. The Orthomosaic has uniform scale and can be used for 2D measurements (distance, surface). It corrects the following problems of the input images:

a) Perspective of the camera.
b) Different scale based on the distance that each point of the object / ground has from the camera.

Orthomosaic Generation: The Orthomosaic generation is based on orthorectification**.** This method removes the perspective distortions from the images using the 3D model. A high number of matches/keypoints (more than 1000) is required to generate the 3D model. This method handles all types of terrain, as well as large datasets. Distances are preserved and therefore the Orthomosaic can be used for measurements.

The following steps are performed to generate the Orthomosaic:

a) **Input:** Images with perspective (for example: facades are visible, roofs do not have the correct size as the scale is not preserved).
b) **Processing:** Calibrate images and compute 3D model. Project images to generate the Orthomosaic.

c) **Output:** Orthomosaic (similar to satellite imagery, facades are not visible, roofs have the correct size).

Figure 13: Orthomosaic. (Source: Pix4d support)

Distortions and Artifacts in the Orthomosaic: The Orthomosaic is generated based on the DSM that was created from the Densified Point Cloud. Thereby, errors and noise present in the Densified Point Cloud will be reflected in the Orthomosaic.

When computing the Densified Point Cloud, the altitude of the points will not be perfectly estimated. There are always some errors and noise that are minimized for good datasets (high overlap, good visual content of the images, use of GCPs, etc.).

These errors and noise result in altitude differences for points that are supposed to be at the same altitude, such as points that belong to the same roof edge of a building or the same edge of a bridge. This altitude difference explains the distortions that appear in the Orthomosaic on building edges, bridges, etc.

3.5. GENERATION OF MAPS SHOWING THE PAVEMENT DISTRESS

The Orthomosaic generated from Pix4d in the form of geo-tiff format is further exported as a layer in AutoCAD Civil 3D 2015 software. Polylines are drawn using the Orthomosaic as layer and area and perimeter of each of the polylines drawn can be calculated. The polylines which was exported from Pix4d are imported on the geo-referenced Orthomosaic layer so that all the pavement distresses are marked properly. Then, this drawing can be used as a map for the Surveyors or Engineers in-charge or as a progress report for keeping it in their road maintenance work report.

CHAPTER 4

IMPLEMENTATION AND RESULTS

4.1. STUDY AREA

The study area is in **Bhoirymbong**, **Sumer 4 No** and **Umtham** which are under Umsning C and RD Block, Ri Bhoi District, Meghalaya, India. A portion of the roads located in these areas of interest are studied for this project. These roads are classified as Other District Roads (ODR) and consist of various pavement defects like cracks, potholes, ravelling, etc. The maintenance of these roads is under the charge of Public Works Department (PWD) Roads, Government of Meghalaya. However, due to the passage of time, the performances of these roads or pavements have become unfavorable. Proper inspection should be done so that maintenance work can be planned and carried out accordingly. Since the number of pavement defects are many and to improve the current conventional method of manual inspection, either by foot or vehicle, UAV is used for the purpose of Road Condition Survey.

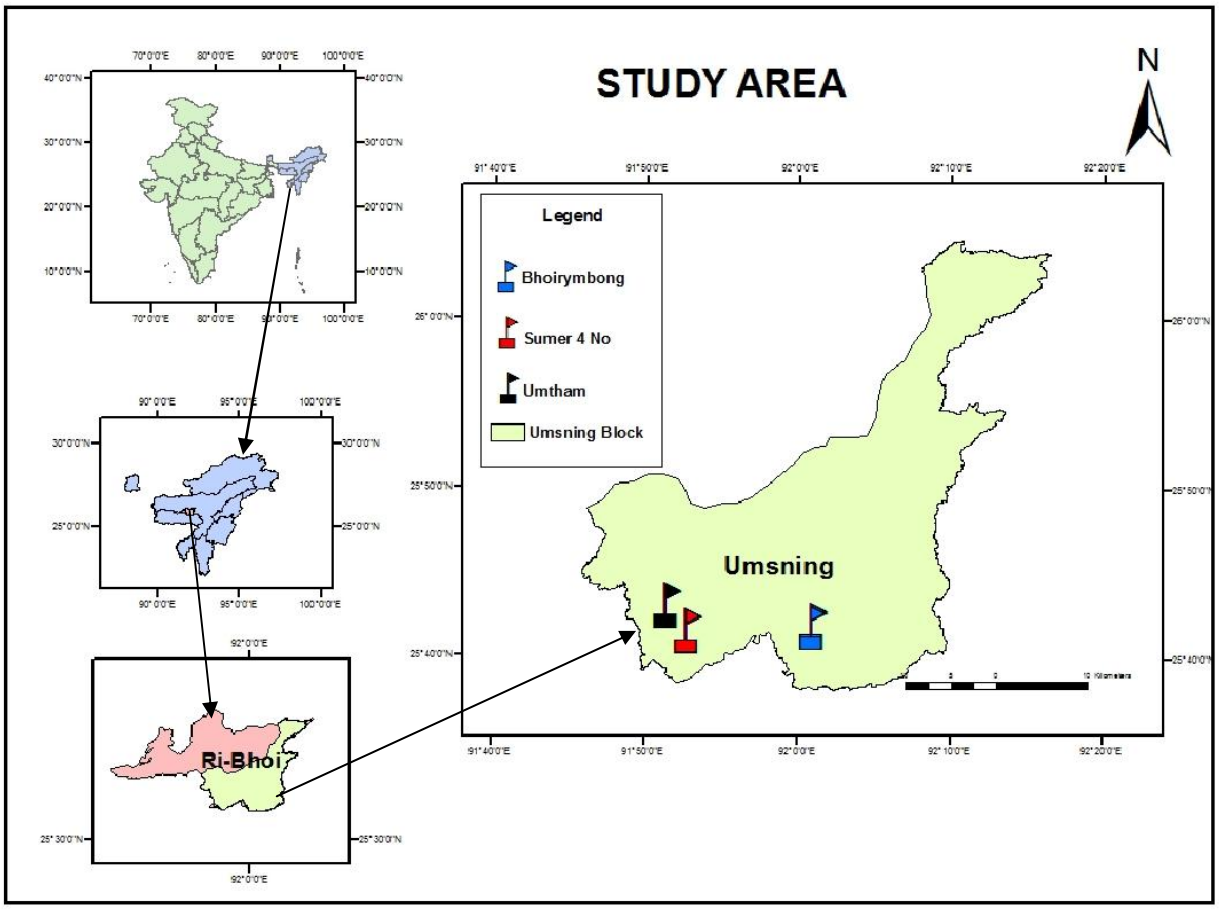

Figure 14: Map of the Study area.

4.2. DATA COLLECTION AND IMAGE PROCESSING IN MATLAB

The UAV is flown in the area of interest and the data collected for this research work is in the form of images. The total duration taken to fly the UAV is less than 30 minutes and at an altitude of 5m and 60m. In this 30 minutes duration, 114 images were taken for the road in Bhoirymbong, 122 images for the road in Sumer 4 No and 60 images for the road in Umtham at an altitude of 5 m. Then, the collected images at 5m altitude are processed using MATLAB software.

i) In the 114 images of the portion of the road in Bhoirymbong, there contained images with defects like cracks, potholes and ravelling.

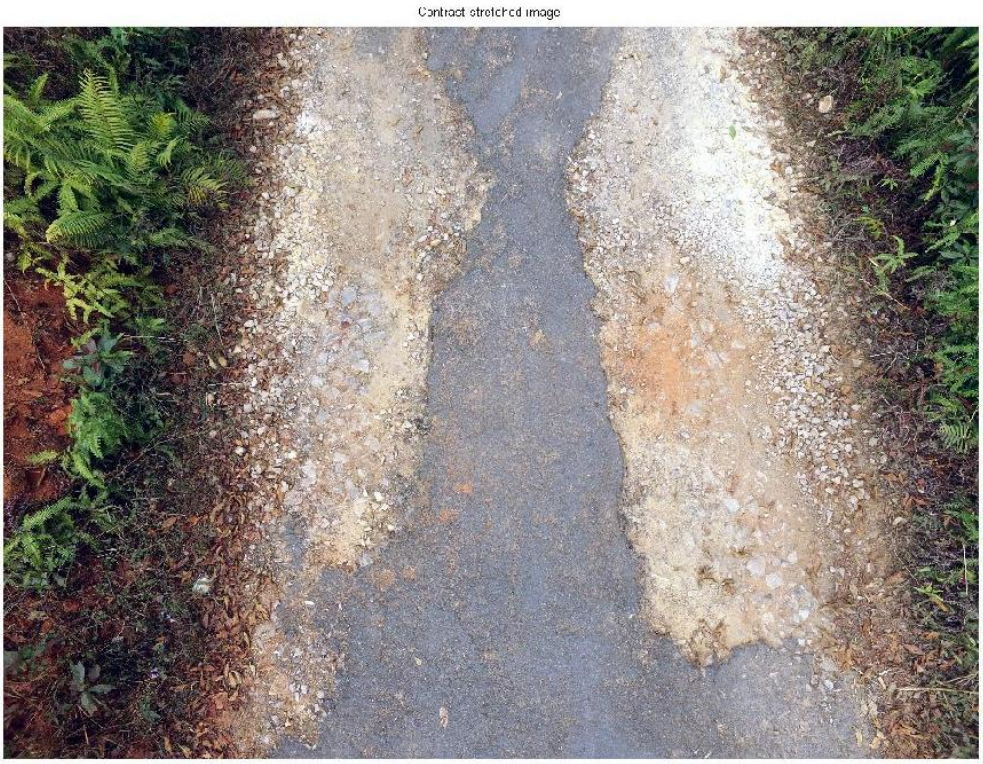

Figure 15.a: UAV image No-10 of Bhoirymbong road.

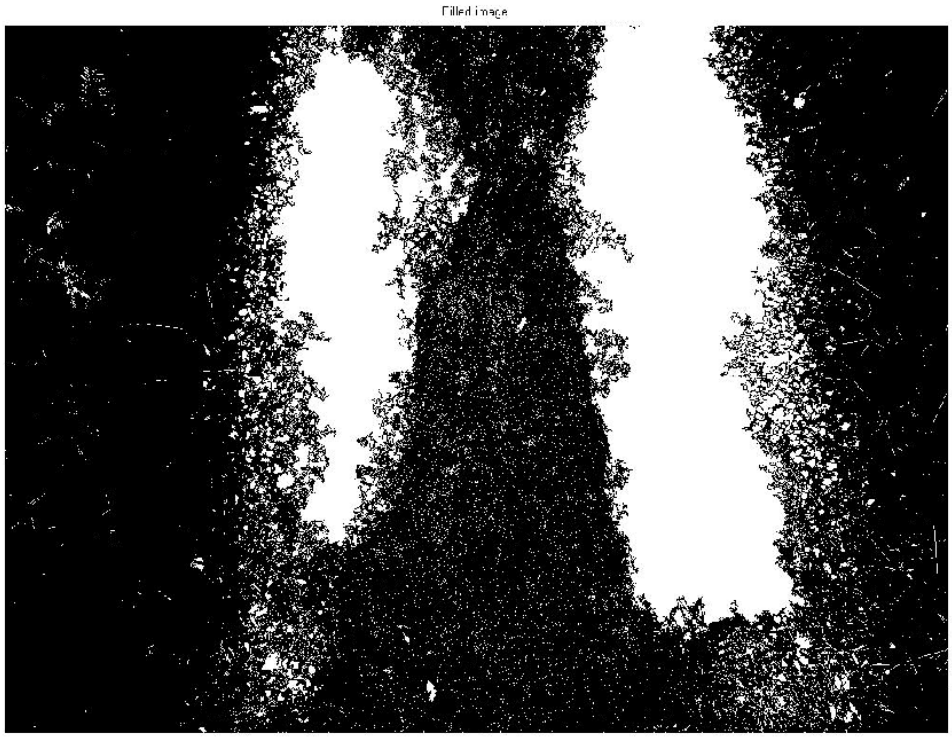

Figure 15.b: Processed UAV image No-10 (Filled Image) of Bhoirymbong road (Threshold used-0.60).

ii) In the 122 images of the portion of the road in Sumer 4 No, there contained images with defects like cracks, depression, potholes, ravelling and shoving.

Figure 16.a: UAV image No-119 of Sumer 4 No road.

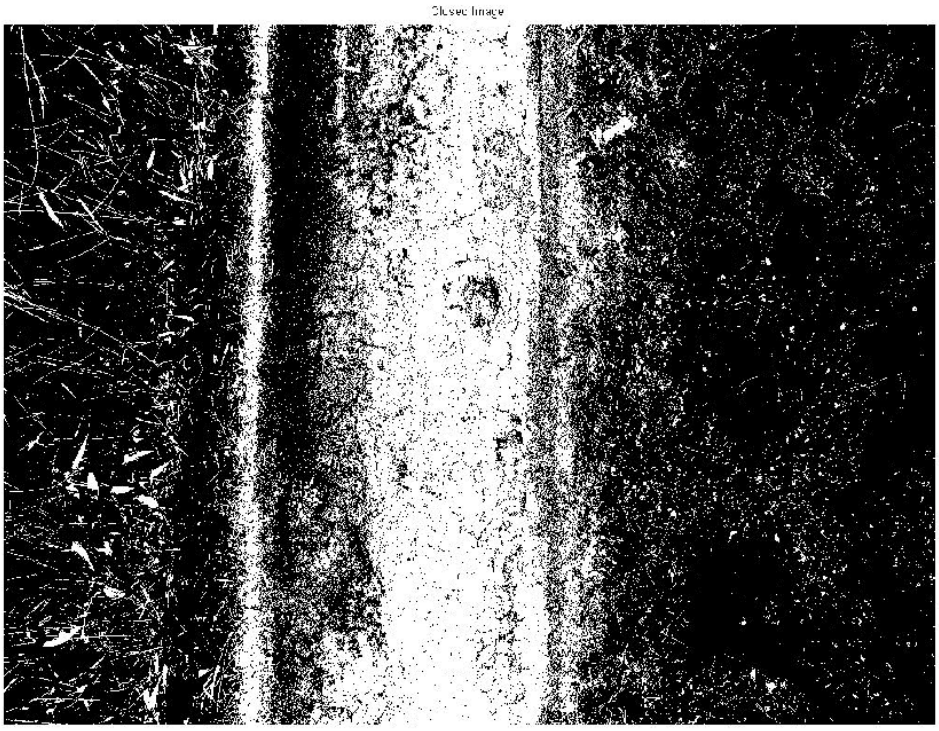

Figure 16.b: Processed UAV image No-119 (Closed Image) of Sumer 4 No road (Threshold used-0.68).

iii) In the 60 images of the portion of the road in Umtham, there contained images with defects like corrugation, depression, potholes, ravelling and unpaved surface.

Figure 17.a: UAV image No-18 of Umtham road.

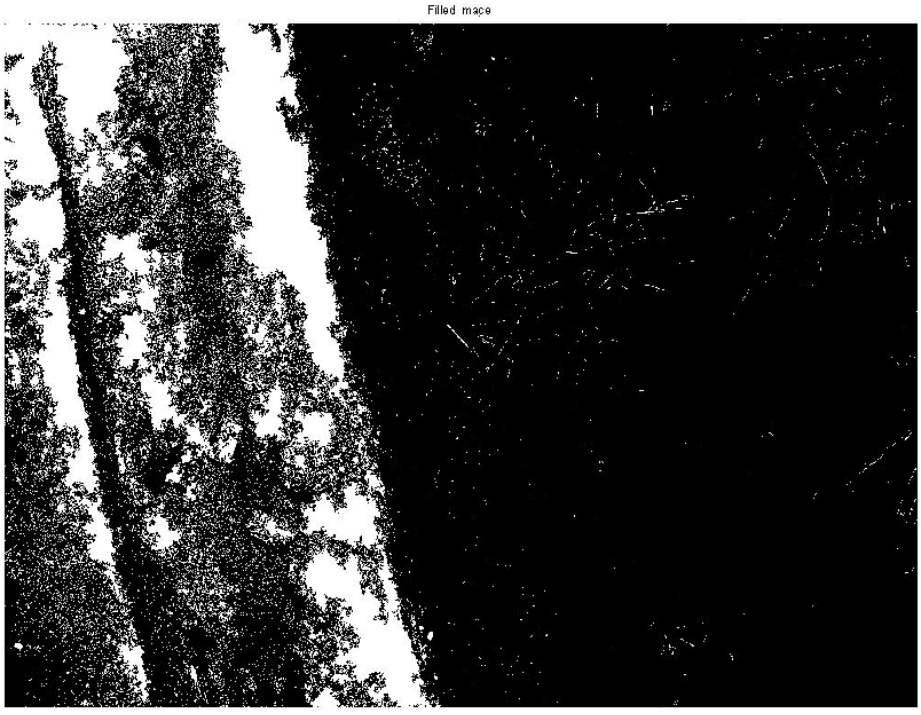

Figure 17.b: Processed UAV image No-18 (Filled Image) of Umtham road (Threshold used-0.70).

After the image processing, from the filled and closed image, the Region of Interest will be created for measuring the pavement distress (in pixels) in order to do the severity analysis.

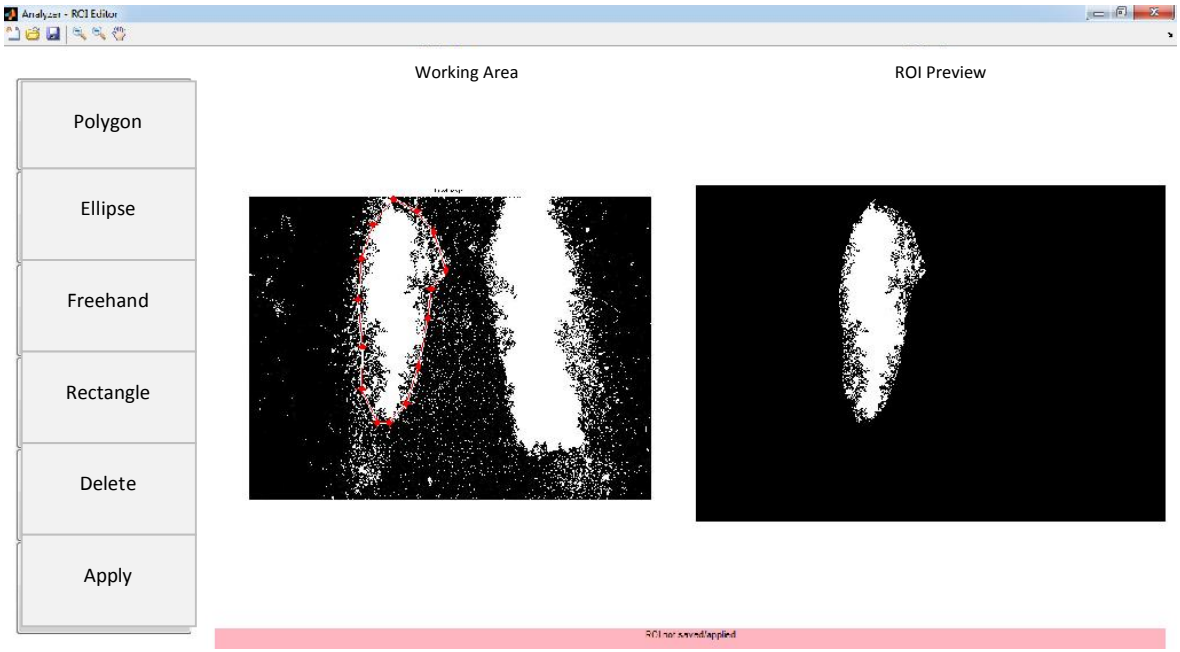

Figure 18: Creating the Region of Interest (ROI) of the pavement distress in MATLAB software.

The different colors represent the independent regions based on the shapes created.

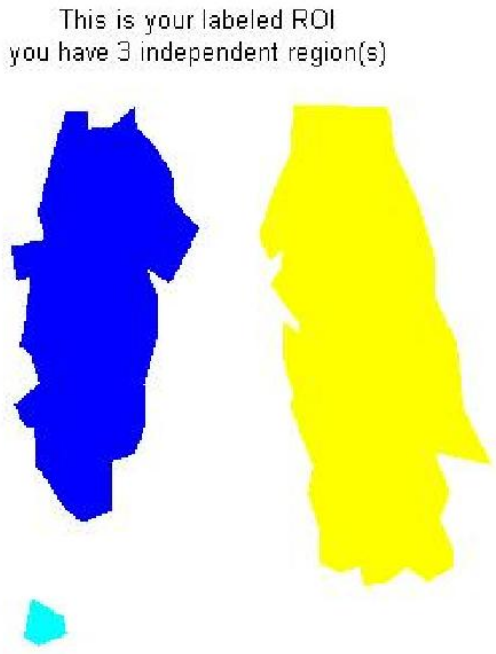

Figure 19.a: Region of Interest (ROI) image of the Pavement distress of Bhoirymbong road.

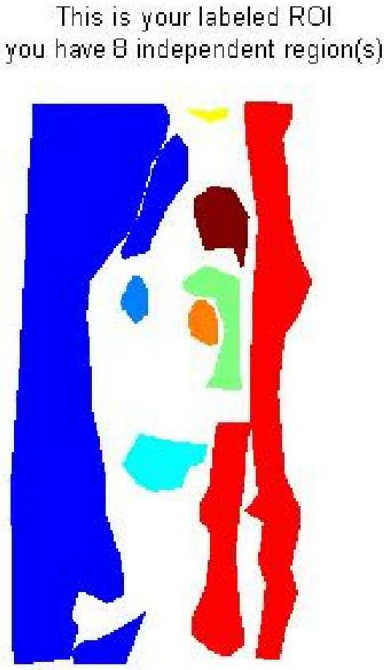

Figure 19.b: Region of Interest (ROI) image of the Pavement distress of Sumer 4 No road.

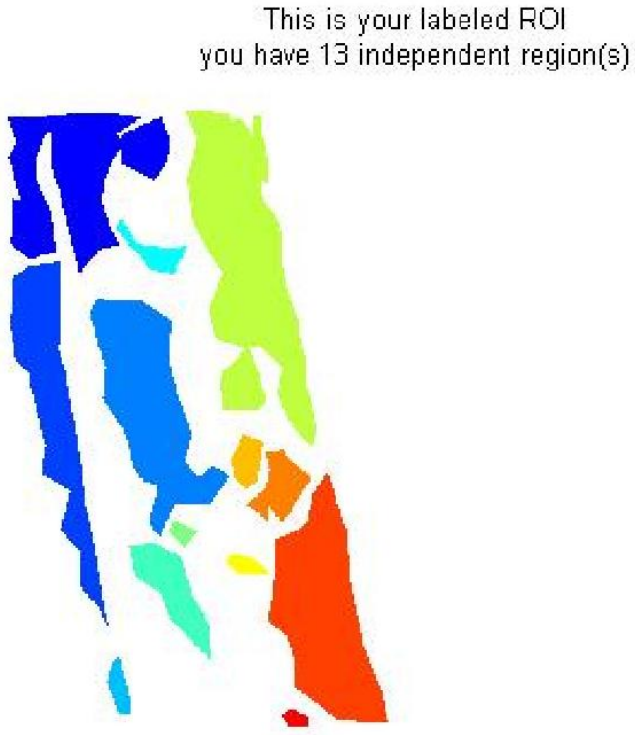

Figure 19.c: Region of Interest (ROI) image of the Pavement distress of Umtham road.

4.3. MEASUREMENT OF PAVEMENT DISTRESS

For measuring pavement distress by conventional method, a long ruler and tape is used and usually two or three levels of severity exist within one distress area. These levels are applied to each defect and are classified as Low, Medium and High Severity and accordingly parameters can be set for these levels. However, for this project, since the data collected from UAV are geo-tagged, the location of these pavement defects can be identified along with the severity level, measured from the ROI image, that is, the image which has the highest pavement distress is considered to be the one with the highest severity level and that, that area or location becomes the highest priority to be repaired or maintained. As per Indian Roads Congress (IRC), the defects are measured in percentage for the Pavement Condition Rating.

Table 3: Pavement Condition Rating based on different types of defects.

DEFECTS	RANGE OF DISTRESS				
Cracking (%)	>30	21 to 30	11 to 20	5 to 10	<5
Ravelling (%)	>30	11 to 30	6 to 10	1 to 5	0
Pothole (%)	>1	0.6 to 1	0.1 to 0.5	0.10	0
Shoving (%)	>1	0.6 to 1	0.1 to 0.5	0.10	0
Patch (%)	>30	16 to 30	6 to 15	2 to 5	<2
Settlement & depression (%)	>5	3 to 5	Up to 2	Up to 1	0
Rutting (mm)	>50	21 to 50	11 to 20	5 to 10	<5
Rating	1	2	3	4	5
Condition	Very Poor	Poor	Fair	Good	Very Good

(Source: Guidelines for Maintenance Management of primary, secondary and urban roads, IRC, 2004)

Due to the geo-tagging properties of the data collected from the UAV, from the list of pavement distress severity or Severity Analysis, the location of the images is marked in Google Earth with the corresponding image attached. This will help the Surveyors or

Engineers-in-charge as an information system. This information system from Google Earth can also be represented in the form of maps.

For the Severity Analysis, from the ROI image, the pavement distress is measured in pixels (Refer Appendix B), but for generating maps with the use of the Orthomosaic (Output from Pix4d software) in AutoCAD Civil 3D 2015, the area of pavement distress is measured in square meters (m^2).

Table 4: List of pavement distress severity in Bhoirymbong road.

Sl no	Pavement distress (pixels)	Image No	Latitude	Longitude
1	13588133	11	25; 41; 47.74	92; 1; 4.87
2	13084833	54	25; 41; 49.996	92; 1; 4.95
3	12980411	55	25; 41; 50.01	92; 1; 4.95
4	12062599	46	25; 41; 49.78	92; 1; 5.06
5	11635739	45	25; 41; 49.78	92; 1; 5.06
6	11010436	42	25; 41; 49.67	92; 1; 5.10
7	10566656	10	25; 41; 47.71	92; 1; 4.85
8	10346665	40	25; 41; 49.43	92; 1; 5.18
9	10293425	48	25; 41; 49.78	92; 1; 5.06
10	9973561	19	25; 41; 47.994	92; 1; 5.01
11	9677740	47	25; 41; 49.78	92; 1; 5.06
12	9591757	52	25; 41; 49.88	92; 1; 5.00
13	9506325	91	25; 41; 51.67	92; 1; 4.82
14	9476391	51	25; 41; 49.84	92; 1; 5.02
15	9117157	53	25; 41; 49.93	92; 1; 4.97
16	8736024	15	25; 41; 47.89	92; 1; 4.95
17	8681391	20	25; 41; 48.02	92; 1; 5.01
18	8626518	50	25; 41; 49.81	92; 1; 5.03
19	8350751	23	25; 41; 48.23	92; 1; 5.07
20	8294558	12	25; 41; 47.82	92; 1; 4.91
21	8260383	49	25; 41; 49.78	92; 1; 5.05
22	8244156	97	25; 41; 52.13	92; 1; 5.00
23	8071088	56	25; 41; 50.11	92; 1; 4.92
24	8059331	25	25; 41; 48.53	92; 1; 5.16
25	7915299	14	25; 41; 47.88	92; 1; 4.94
26	7576607	37	25; 41; 49.14	92; 1; 5.20

27	7346462	90	25; 41; 51.58	92; 1; 4.78
28	7222038	9	25; 41; 47.67	92; 1; 4.83
29	7206309	67	25; 41; 50.58	92; 1; 4.73
30	7124416	43	25; 41; 49.76	92; 1; 5.07
31	7066096	22	25; 41; 48.15	92; 1; 5.04
32	6946089	8	25; 41; 47.63	92; 1; 4.80
33	6938474	24	25; 41; 48.38	92; 1; 5.12
34	6738002	58	25; 41; 50.19	92; 1; 4.89
35	6731090	102	25; 41; 52.44	92; 1; 5.26
36	6516598	26	25; 41; 48.56	92; 1; 5.16
37	6416000	44	25; 41; 49.78	92;1; 5.06
38	6298693	35	25; 41; 48.97	92; 1; 5.22
39	6273956	94	25; 41; 51.85	92; 1; 4.92
40	6261970	76	25; 41; 51.11	92; 1; 4.69
41	6237037	13	25; 41; 47.88	92; 1; 4.95
42	6026735	63	25; 41; 50.40	92; 1; 4.82
43	6025941	7	25; 41; 47.60	92; 1; 4.78
44	5963589	59	25; 41; 50.19	92; 1; 4.89
45	5947770	18	25; 41; 47.997	92; 1; 5.013
46	5875399	21	25; 41; 48.10	92; 1; 5.02
47	5857834	98	25; 41; 52.17	92; 1; 5.02
48	5779830	17	25; 41; 47.99	92; 1; 5.00
49	5777201	16	25; 41; 47.96	92; 1; 4.99
50	5722033	85	25; 41; 51.21	92; 1; 4.70
51	5664209	41	25; 41; 49.54	92; 1; 5.14
52	5654641	92	25; 41; 51.72	92; 1; 4.85
53	5577263	66	25; 41; 50.55	92; 1; 4.74
54	5570803	113	25; 41; 53.01	92; 1; 5.63
55	5533975	39	25; 41; 49.39	92; 1; 5.19
56	5498192	93	25; 41; 51.76	92; 1; 4.87
57	5446860	27	25; 41; 48.65	92; 1; 5.19
58	5423596	65	25; 41; 50.49	92; 1; 4.77
59	5375351	29	25; 41; 48.74	92; 1; 5.22
60	5130604	74	25; 41; 50.98	92; 1; 4.69
61	5126700	38	25; 41; 49.31	92; 1; 5.198
62	4958024	64	25; 41; 50.43	92; 1; 4.80
63	4944458	68	25; 41; 50.66	92; 1; 4.70
64	4936806	30	25; 41; 48.76	93; 1; 5.226

65	4921652	75	25; 41; 51.04	92; 1; 4.69
66	4812462	28	25; 41; 48.72	92; 1; 5.21
67	4807269	60	25; 41; 50.19	92; 1; 4.89
68	4681746	6	25; 41; 47.53	92; 1; 4.75
69	4460651	36	25; 41; 49.09	92; 1; 5.21
70	4326194	69	25; 41; 50.80	92; 1; 4.67
71	4308407	86	25; 41; 51.22	92; 1; 4.69
72	4212686	88	25; 41; 51.39	92; 1; 4.72
73	4176253	31	25; 41; 48.78	92; 1; 5.22
74	4154966	34	25; 41; 48.86	92; 1; 5.22
75	4090841	57	25; 41; 50.18	92; 1; 4.89
76	3996752	108	25; 41; 52.63	92; 1; 5.36
77	3850723	89	25; 41; 51.48	92; 1; 4.74
78	3759332	101	25; 41; 52.31	92; 1; 5.15
79	3733643	4	25; 41; 47.52	92; 1; 4.745
80	3684459	33	25; 41; 48.845	92; 1; 5.215
81	3684162	70	25; 41; 50.825	92; 1; 4.671
82	3659414	87	25; 41; 51.32	92; 1; 4.72
83	3639188	103	25; 41; 52.58	92; 1; 5.38
84	3586202	111	25; 41; 52.97	92; 1; 5.57
85	3534089	114	25; 41; 53.05	92; 1; 5.71
86	3514040	104	25; 41; 52.599	92; 1; 5.39
87	3489489	96	25; 41; 51.98	92; 1; 4.945
88	3487969	77	25; 41; 51.13	92; 1; 4.69
89	3479944	112	25; 41; 52.98	92; 1; 5.58
90	3433534	32	25; 41; 48.83	92; 1; 5.21
91	3291727	61	25; 41; 50.19	92; 1; 4.89
92	3178629	95	25; 41; 51.94	92; 1; 4.94
93	3159991	72	25; 41; 50.89	92; 1; 4.68
94	3114917	78	25; 41; 51.13	92; 1; 4.69
95	2927040	99	25; 41; 52.24	92; 1; 5.08
96	2781013	83	25; 41; 51.21	92; 1; 4.726
97	2761791	80	25; 41; 51.21	92; 1; 4.725
98	2729165	5	25; 41; 47.514	92; 1; 4.747
99	2715962	79	25; 41; 51.17	92; 1; 4.71
100	2700119	109	25; 41; 52.69	92; 1; 5.3997
101	2691131	84	25; 41; 51.21	92; 1; 4.72
102	2642671	2	25; 41; 47.50	92; 1; 4.74

103	2616642	100	25; 41; 52.26	92; 1; 5.101
104	2590641	71	25; 41; 50.834	92; 1; 4.671
105	2580164	73	25; 41; 50.94	92; 1; 4.69
106	2429798	82	25; 41; 51.2137	92; 1; 4.7231
107	2401729	62	25; 41; 50.274	92; 1; 4.867
108	2382231	110	25; 41; 52.86	92; 1; 5.51
109	2347099	81	25; 41; 51.2118	92; 1; 4.725
110	2179842	3	25; 41; 47.514	92; 1; 4.744
111	2128682	106	25; 41; 52.61	92; 1; 5.39
112	2072087	1	25; 41; 47.44	92; 1; 4.72
113	2042874	105	25; 41; 52.61	92; 1; 5.40
114	1814782	107	25; 41; 52.61	92; 1; 5.395

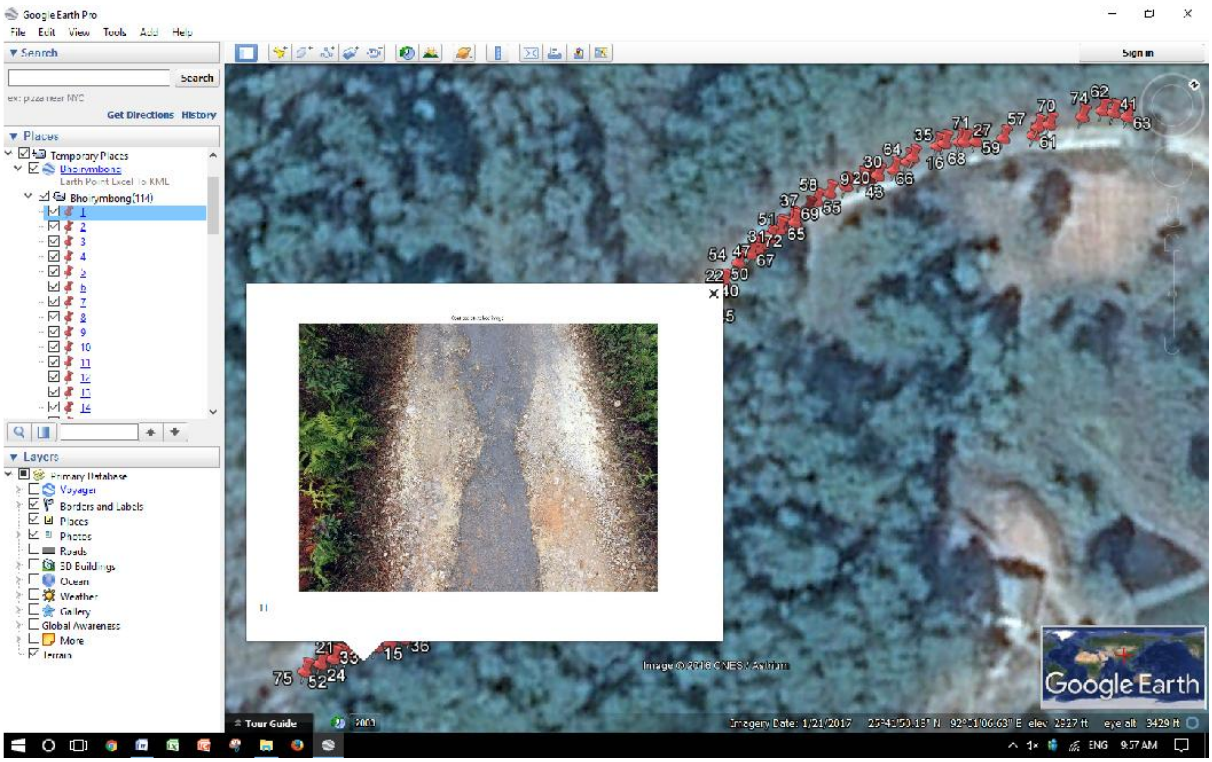

Figure 20: Site- Bhoirymbong. Highest Severity of pavement distress.

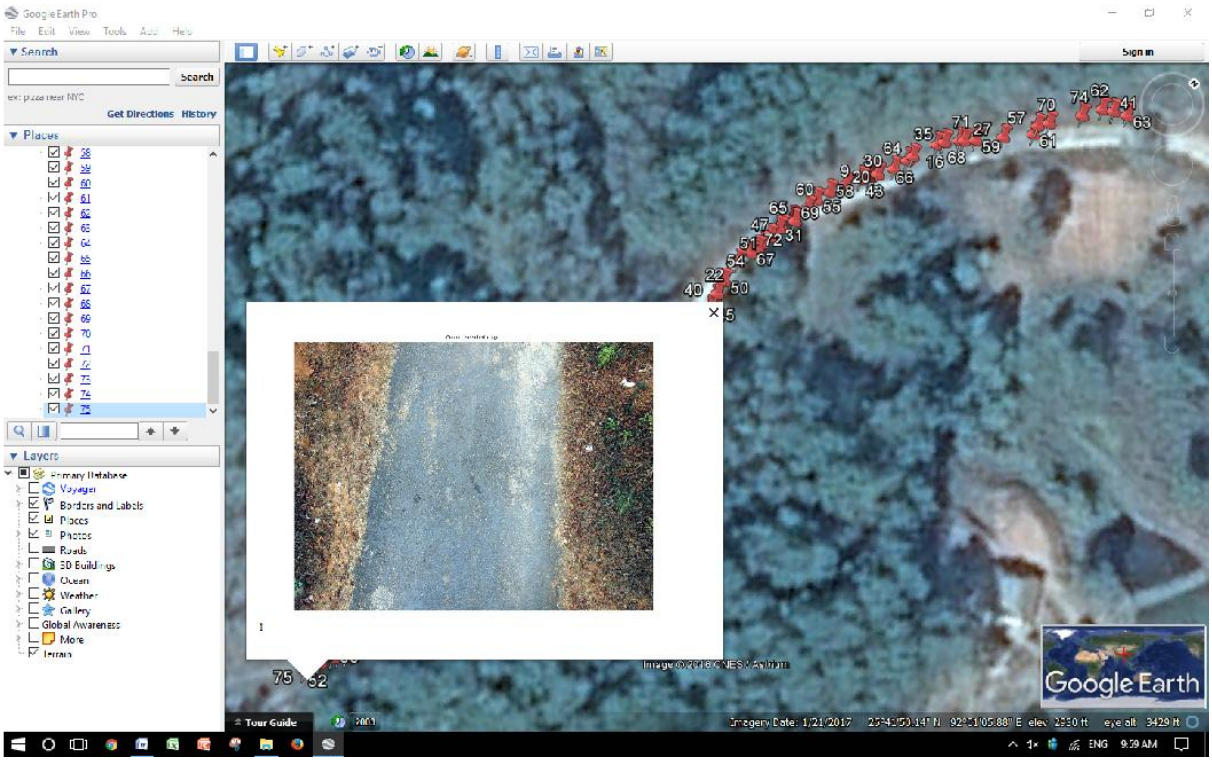

Figure 21: Site- Bhoirymbong. Lowest severity of pavement distress.

Figure 22: Site-Bhoirymbong. Road distress location.

Figure 23: Site-Bhoirymbong. Path where the UAV was flown.

Table 5: List of pavement distress severity in Sumer 4 No road.

Sl no	Pavement distress (pixels)	Image No	Latitude	Longitude
1	12731796	120	25; 41; 30.94	91; 52; 53.79
2	12276525	119	25; 41; 30.95	91; 52; 53.78
3	10337166	122	25; 41; 30.94	91; 52; 53.79
4	8619630	121	25; 41; 30.94	91; 52; 53.79
5	6677496	118	25; 41; 30.91	91; 52; 53.61
6	6487515	117	25; 41; 30.85	91; 52; 53.39
7	5980949	116	25; 41; 30.82	91; 52; 53.24
8	5867110	32	25; 41; 32.92	91; 52; 50.94
9	5673497	31	25; 41; 32.93	91; 52; 50.94
10	5664960	5	25; 41; 34.47	91; 52; 51.23
11	5345861	24	25; 41; 33.21	91; 52; 51.11
12	5179562	115	25; 41; 30.80	91; 52; 53.12
13	5175660	27	25; 41; 33.145	91; 52; 51.01
14	4872695	21	25; 41; 33.366	91; 52; 51.178
15	4856484	28	25; 41; 33.14	91; 52; 51.01
16	4709276	26	25; 41; 33.14	91; 52; 51.06

17	4484544	41	25; 41; 32.51	91; 52; 50.81
18	4467697	30	25; 41; 33.03	91; 52; 50.97
19	4432323	29	25; 41; 33.06	91; 52; 50.98
20	4256835	23	25; 41; 33.34	91; 52; 51.18
21	4246535	25	25; 41; 33.15	91; 52; 51.10
22	3934511	22	25; 41; 33.36	91; 52; 51.18
23	3858413	33	25; 41; 32.83	91; 52; 50.93
24	3760869	61	25; 41; 31.42	91; 52; 51.56
25	3676094	60	25; 41; 31.42	91; 52; 51.55
26	3608120	2	25; 41; 34.55	91; 52; 51.21
27	3600013	8	25; 41; 34.18	91; 52; 51.28
28	3596965	36	25; 41; 32.72	91; 52; 50.86
29	3537556	74	25; 41; 30.78	91; 52; 52.07
30	3517805	107	25; 41; 30.71	91; 52; 52.32
31	3517202	7	25; 41; 34.28	91; 52; 51.30
32	3495060	101	25; 41; 30.71	91; 52; 52.29
33	3483065	18	25; 41; 33.64	91; 52; 51.30
34	3466475	17	25; 41; 33.71	91; 52; 51.30
35	3347645	1	25; 41; 34.546	91; 52; 51.21
36	3271496	75	25; 41; 30.73	91; 52; 52.17
37	3161632	63	25; 41; 31.33	91; 52; 51.60
38	3068529	59	25; 41; 31.42	91; 52; 51.56
39	3059229	9	25; 41; 34.18	91; 52; 51.28
40	3049389	3	25; 41; 34.55	91; 52; 51.22
41	3040587	73	25; 41; 30.826	91; 52; 51.992
42	3029783	104	25; 41; 30.71	91; 52; 52.285
43	2925175	42	25; 41; 31.87	91; 52; 51.26
44	2726073	20	25; 41; 33.53	91; 52; 51.24
45	2711514	103	25; 41; 30.71	91; 52; 52.285
46	2692728	58	25; 41; 31.43	91; 52; 51.56
47	2689600	98	25; 41; 30.71	91; 52; 52.28
48	2655352	62	25; 41; 31.37	91; 52; 51.60
49	2639764	4	25; 41; 34.546	91; 52; 51.21
50	2610413	85	25; 41; 30.79	91; 52; 52.88
51	2609086	64	25; 41; 31.33	91; 52; 51.606
52	2568999	35	25; 41; 32.76	91; 52; 50.89
53	2554029	114	25; 41; 30.75	91; 52; 52.96
54	2538463	113	25; 41; 30.73	91; 52; 52.86

55	2537202	83	25; 41; 30.79	91; 52; 52.88
56	2502101	94	25; 41; 30.75	91; 52; 52.53
57	2501282	6	25; 41; 34.36	91; 52; 51.27
58	2490214	34	25; 41; 32.79	91; 52; 50.92
59	2479518	111	25; 41; 30.68	91; 52; 52.69
60	2477232	96	25; 41; 30.71	91; 52; 52.36
61	2458775	106	25; 41; 30.71	91; 52; 52.29
62	2455046	99	25; 41; 30.71	91; 52; 52.28
63	2386473	10	25; 41; 31.13	91; 52; 51.28
64	2360224	86	25; 41; 30.79	91; 52; 52.88
65	2338073	93	25; 41; 30.746	91; 52; 52.53
66	2262411	82	25; 41; 30.79	91; 52; 52.87
67	2244405	108	25; 41; 30.71	91; 52; 52.45
68	2237340	112	25; 41; 30.69	91; 52; 52.73
69	2225534	102	25; 41; 30.71	91; 52; 52.28
70	2214341	57	25; 41; 31.43	91; 52; 51.56
71	2208227	46	25; 41; 31.87	91; 52; 51.26
72	2202391	49	25; 41; 31.89	91; 52; 51.32
73	2190105	97	25; 41; 30.71	91; 52; 52.29
74	2140166	70	25; 41; 31.00	91; 52; 51.81
75	2124091	47	25; 41; 31.87	91; 52; 51.26
76	2106698	19	25; 41; 33.58	91; 52; 51.26
77	2089608	56	25; 41; 31.46	91; 52; 51.53
78	2069021	87	25; 41; 30.79	91; 52; 52.866
79	2042481	48	25; 41; 31.90	91; 52; 51.31
80	2022504	100	25; 41; 30.71	91; 52; 52.28
81	2018342	105	25; 41; 30.71	91; 52; 52.29
82	1966522	16	25; 41; 33.83	91; 52 51.30
83	1882342	78	25; 41; 30.62	91; 52; 52.586
84	1879741	84	25; 41; 30.79	91; 52; 52.88
85	1874614	88	25; 41; 30.78	91; 52; 52.82
86	1846218	76	25; 41; 30.70	91; 52; 52.24
87	1841900	65	25; 41; 31.25	91; 52; 51.66
88	1709056	15	25; 41; 33.846	91; 52; 51.295
89	1706454	110	25; 41; 30.69	91; 52; 52.62
90	1681855	11	25; 41; 34.08	91; 52; 51.26
91	1641339	90	25; 41; 30.79	91; 52; 52.78
92	1626194	109	25; 41; 30.70	91; 52; 52.48

93	1586260	72	25; 41; 30.86	91; 52; 51.96
94	1580558	91	25; 41; 30.78	91; 52; 52.73
95	1565600	43	25; 41; 31.87	91; 52; 51.26
96	1553910	89	25; 41; 30.785	91; 52; 52.795
97	1538951	40	25; 41; 32.51	91; 52; 50.81
98	1522277	44	25; 41; 31.87	91; 52; 51.26
99	1501238	45	25; 41; 31.87	91; 52; 51.26
100	1436184	71	25; 41; 30.965	91; 52; 51.85
101	1423632	80	25; 41; 30.69	91; 52; 52.62
102	1346755	81	25; 41; 30.74	91; 52; 52.74
103	1319115	92	25; 41; 30.75	91; 52; 52.61
104	1273429	79	25; 41; 30.66	91; 52; 52.60
105	1270899	77	25; 41; 30.64	91; 52; 52.47
106	1111473	50	25; 41; 31.80	91; 52; 51.37
107	1085485	52	25; 41; 31.66	91; 52; 51.42
108	1076451	66	25; 41; 31.18	91; 52; 51.72
109	956659	53	25; 41; 31.64	91; 52; 51.43
110	954222	14	25; 41; 33.90	91; 52; 51.29
111	936467	95	25; 41; 30.74	91; 52; 52.49
112	767599	12	25; 41; 33.99	91; 52; 51.27
113	752734	51	25; 41; 31.73	91; 52; 51.39
114	678797	55	25; 41; 31.526	91; 52; 51.49
115	651083	69	25; 41; 31.09	91; 52; 51.73
116	635293	54	25; 41; 31.55	91; 52; 51.47
117	493385	13	25; 41; 33.90	91; 52; 51.28
118	441701	37	25; 41; 32.59	91; 52; 50.88
119	339340	68	25; 41; 31.11	91; 52; 51.73
120	121301	67	25; 41; 31.13	91; 52; 51.73
121	0	38	25; 41; 32.54	91; 52; 50.90
		39	25; 41; 32.53	91; 52; 50.90

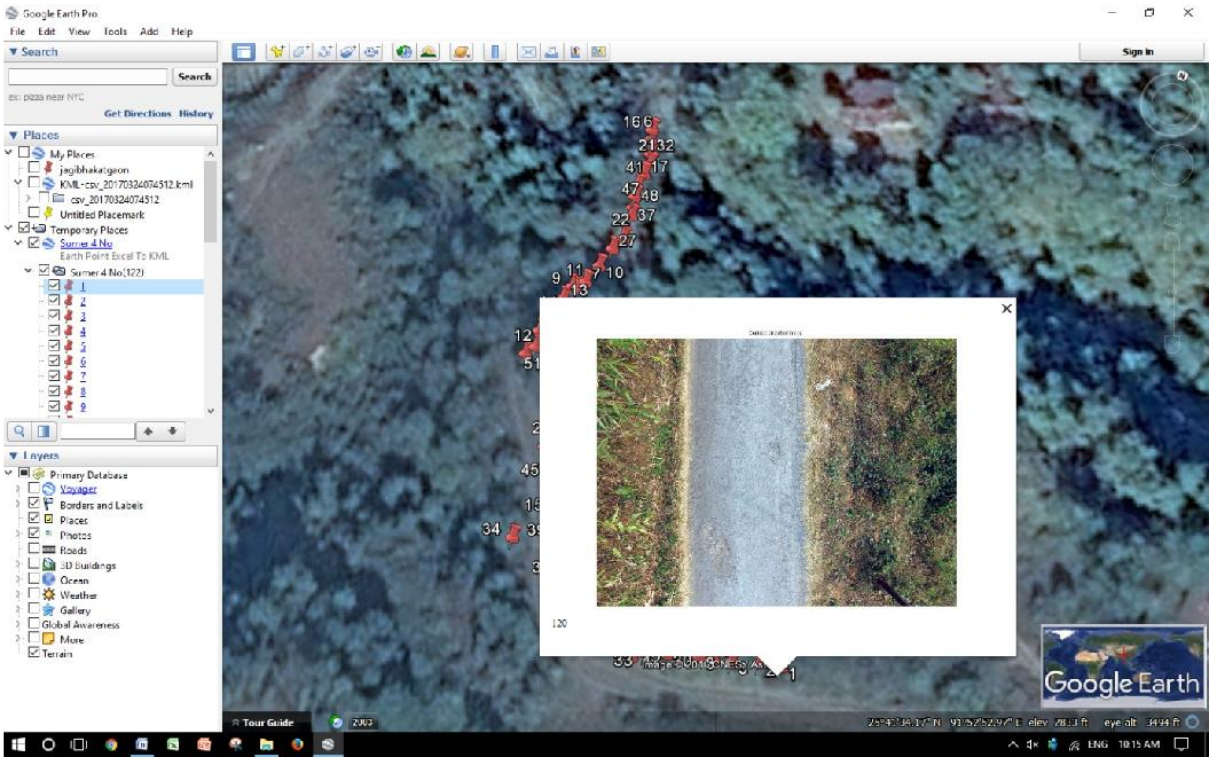

Figure 24: Site- Sumer 4 No. Highest severity pavement distress.

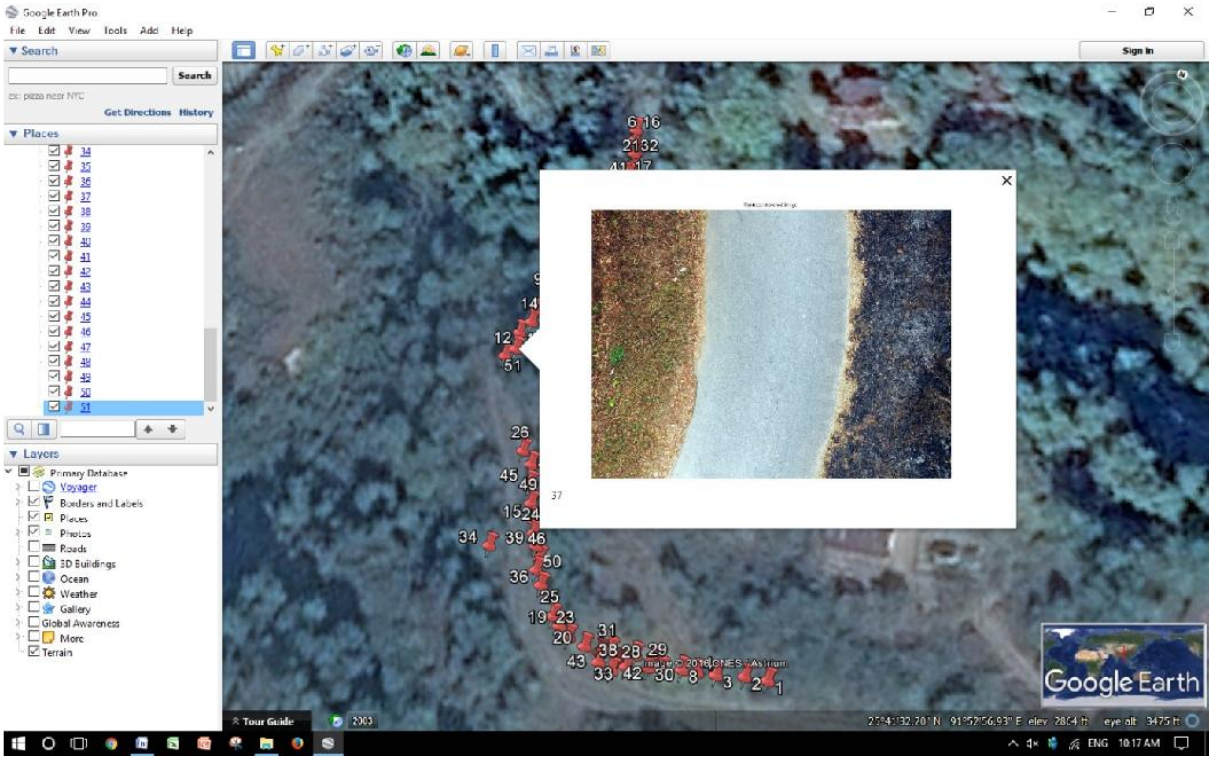

Figure 25: Site- Sumer 4 No. Lowest severity pavement distress.

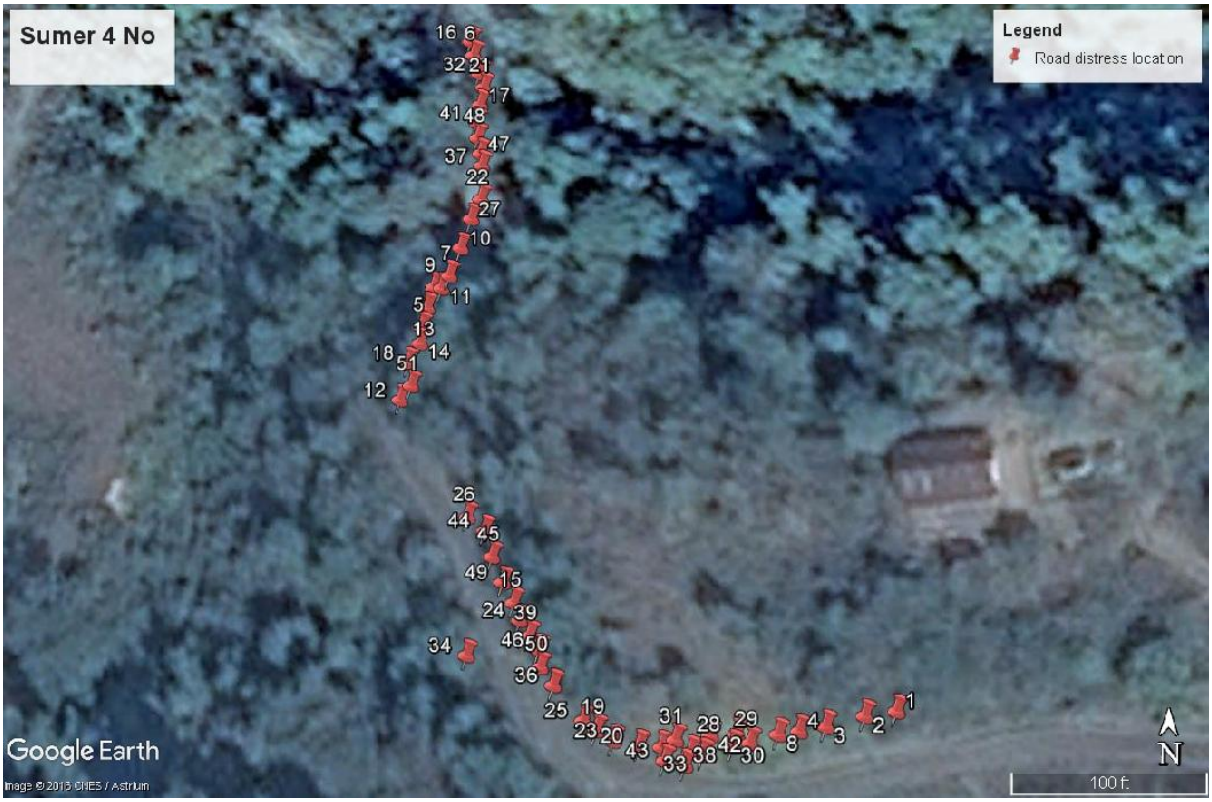

Figure 26: Site- Sumer 4 No. Road distress location.

Figure 27: Site-Sumer 4 No. Path where the UAV was flown.

Table 6: List of pavement distress severity in Umtham road.

Sl no	Pavement distress (pixels)	Image No	Latitude	Longitude
1	16092881	35	25; 43; 3.78	91; 51; 29.26
2	15290488	40	25; 43; 3.72	91; 51; 29.27
3	14289238	38	25; 43; 3.73	91; 51; 29.24
4	13499956	33	25; 43; 3.78	91; 51; 29.27
5	12852758	53	25; 43; 2.66	91; 51; 28.76
6	12709020	36	25; 43; 3.77	91; 51; 29.28
7	12374473	27	25; 43; 2.48	91; 51; 28.78
8	12263731	29	25; 43; 2.53	91; 51; 28.81
9	11934940	39	25; 43; 3.74	91; 51; 29.23
10	11695934	34	25; 43; 3.76	91; 51; 29.26
11	11493265	30	25; 43; 2.53	91; 51; 28.81
12	11485183	37	25; 43; 3.76	91; 51; 29.28
13	11190938	58	25; 43; 2.56	91; 51; 28.703
14	10935872	55	25; 43; 2.63	91; 51; 28.75
15	10715740	56	25; 43; 2.585	91; 51; 28.722
16	10669969	52	25; 43; 2.70	91; 51; 28.798
17	10028375	57	25; 43; 2.56	91; 51; 28.706
18	9806287	43	25; 43; 3.24	91; 51; 29.024
19	9659996	28	25; 43; 2.53	91; 51; 28.811
20	9606745	26	25; 43; 2.402	91; 51; 28.75
21	9489323	54	25; 43; 2.65	91; 51; 28.76
22	9374679	32	25; 43; 3.787	91; 51; 29.266
23	9147984	47	25; 43; 2.945	91; 51; 28.922
24	8969940	59	25; 43; 2.56	91; 51; 28.703
25	8792613	31	25; 43; 2.532	91; 51; 28.804
26	8215215	17	25; 43; 1.511	91; 51; 28.394
27	8197635	24	25; 43; 2.39	91; 51; 28.736
28	7948331	5	25; 43; 1.525	91; 51; 28.30
29	7633373	18	25; 43; 1.596	91; 51; 28.44
30	7548317	50	25; 43; 2.814	91; 51; 28.884
31	7434447	1	25; 43; 1.583	91; 51; 28.352
32	7287366	19	25; 43; 1.68	91; 51; 28.4882
33	7004440	25	25; 43; 2.393	91; 51; 28.741
34	6969725	16	25; 43; 1.499	91; 51; 28.38
35	6807092	51	25; 43; 2.75	91; 51; 28.84

36	6798784	48	25; 43; 2.9214	91.51.28.932
37	6468024	6	25; 43; 1.472	91; 51; 28.264
38	6460331	4	25; 43; 1.547	91; 51; 28.311
39	6415876	15	25; 43; 1.483	91; 51; 28.36
40	6401614	7	25; 43; 1.38	91; 51; 28.184
41	6285067	49	25; 43; 2.903	91.51; 28.924
42	6103391	60	25; 43; 2.565	91; 51; 28.704
43	5916981	3	25; 43; 1.58	91; 51; 28.354
44	5803527	42	25; 43; 3.33	91; 51; 29.07
45	5683732	41	25; 43; 3.343	91; 51; 29.108
46	5682055	2	25;43; 1.58	91; 51; 28.36
47	5519404	10	25; 43; 1.32	91; 51; 28.15
48	5146757	20	25; 43; 1.73	91; 51; 28.52
49	5051949	46	25; 43; 3.01	91; 51; 28.88
50	4910653	23	25; 43; 2.37	91; 51; 28.76
51	4747441	14	25; 43; 1.387	91; 51; 28.29
52	4747061	8	25; 43; 1.325	91; 51; 28.152
53	4668417	44	25; 43; 3.17	91; 51; 28.98
54	4487187	21	25; 43; 1.76	91; 51; 28.53
55	4439375	11	25; 43; 1.34	91; 51; 28.25
56	4395582	13	25; 43; 1.34	91; 51; 28.252
57	4049705	45	25; 43; 3.04	91; 51; 28.90
58	3537255	22	25; 43; 1.84	91; 51; 28.585
59	3220438	9	25; 43; 1.32	91; 51; 28.16
60	2350256	12	25; 43; 1.34	91; 51; 28.25

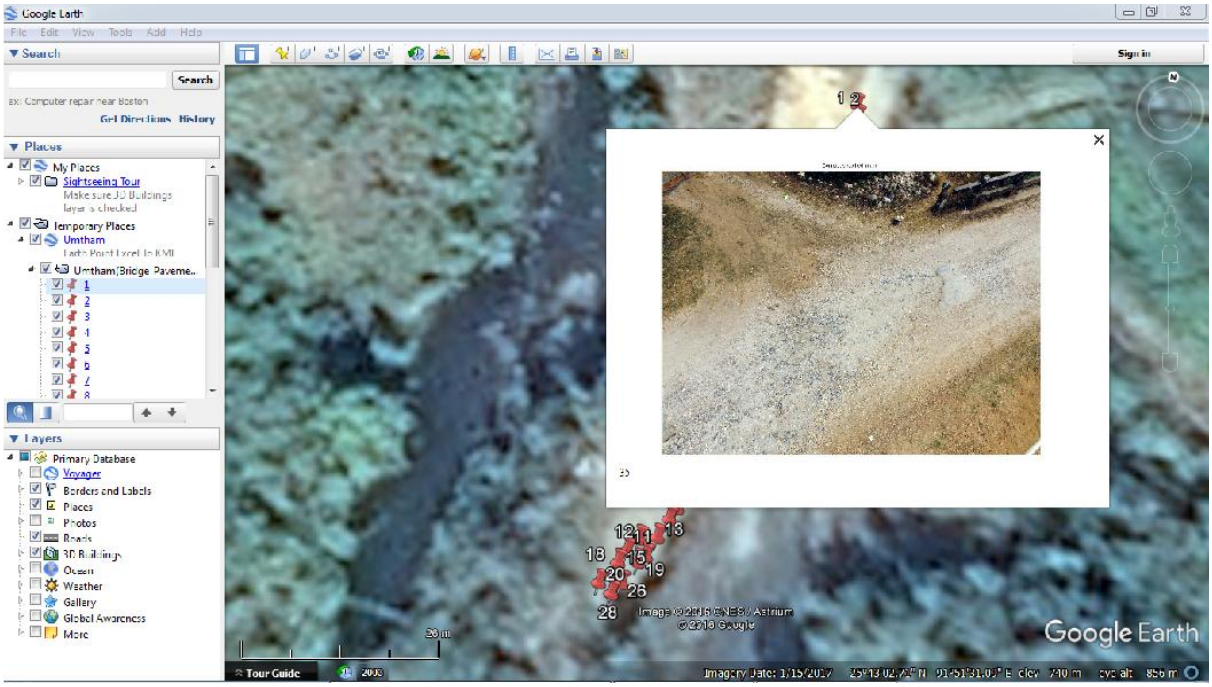

Figure 28: Site- Umtham. Highest Severity pavement distress.

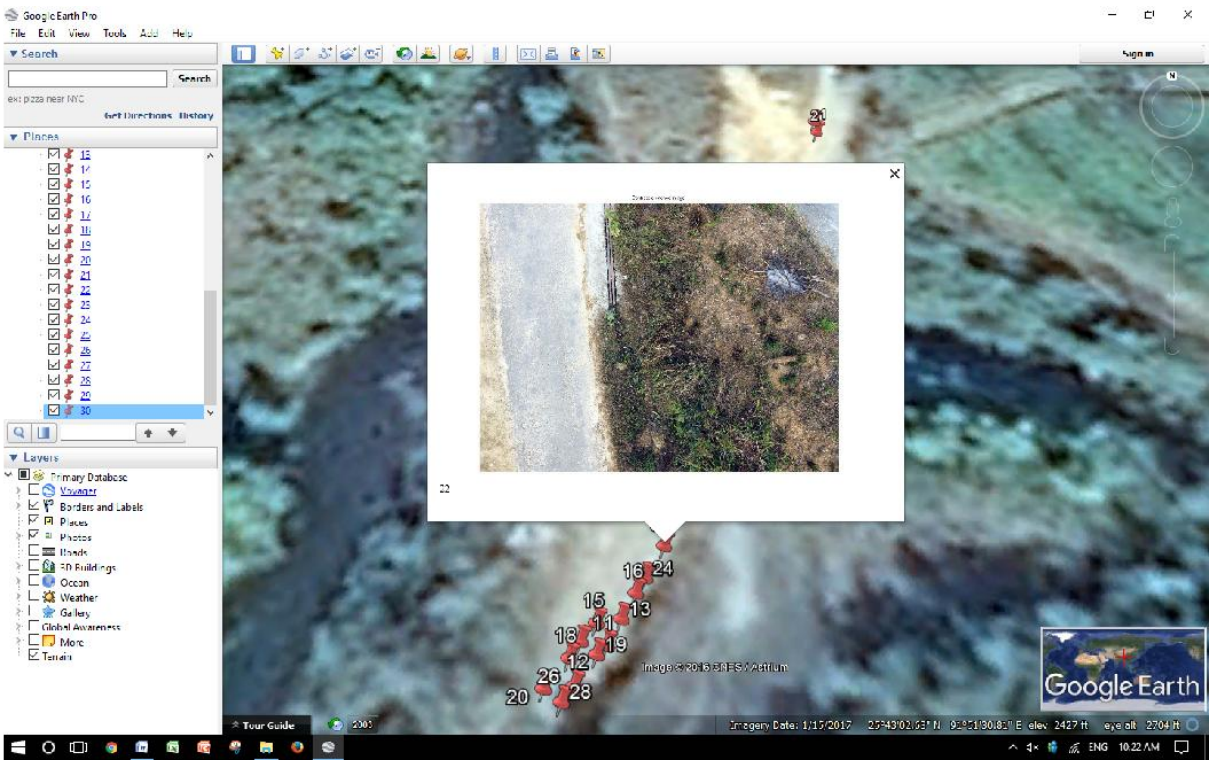

Figure 29: Site-Umtham. Lowest severity pavement distress.

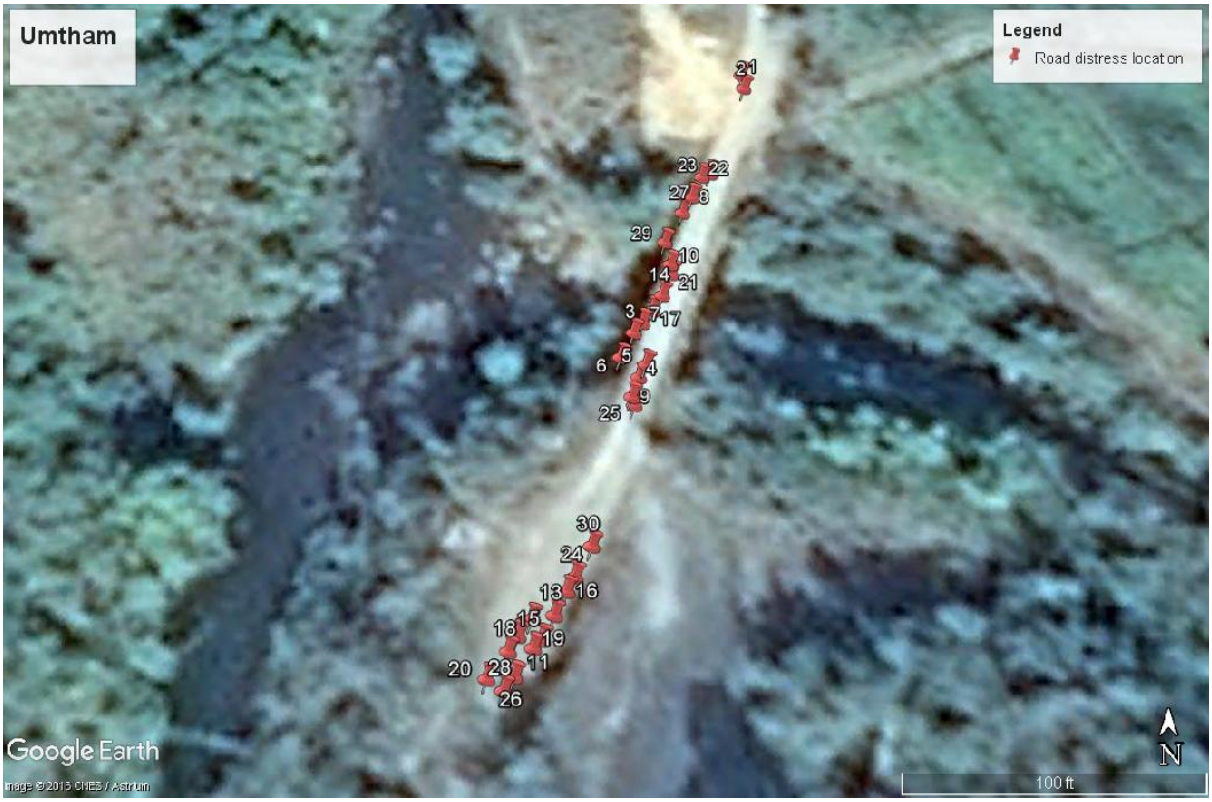

Figure 30: Site-Umtham. Road distress location.

Figure 31: Site-Umtham. Path where the UAV was flown.

4.4. METHOD PERFORMANCE FOR THE TEST OF IMAGES

The analysis of the performance of the method used in MATLAB software is done manually by comparing the original UAV image with the processed image, that is, the Closed image and Filled image. From the analysis, the method used gave the following results:

Table 7: Statistical pavement defects detection results.

Category	Bhoirymbong	Umtham	Sumer 4 No.
TP	144	70	162
FP	13	1	1
TN	0	0	3
FN	64	18	44

Table 8: Method performance for the test of images.

SITE	Bhoirymbong	Umtham	Sumer 4 No.
Precision (%)	91.72	98.59	99.39
Recall (%)	69.23	79.54	78.64
Tracking Accuracy (%)	65.16	78.65	78.57

4.5. PROCESSING IN PIX4D SOFTWARE

While collecting data with the help of UAV, images taken at a fixed altitude of 60 m was also obtained. In **Bhoirymbong**- 77 images, **Sumer 4 No**-48 images and a segment of the road in **Umtham**- 15 images. Accordingly, the area of interest or site were divided into three projects for processing in Pix4d software, i.e, bhoirymbong_h for Bhoirymbong, sumer_roadh for Sumer 4 No and bsite for the segment of the road in Umtham. There are three steps of processing:-

i) **Initial processing**- The quality check of the images is done which includes camera optimization, matching keypoints and geo-referencing the images. Overlapping and block bundle adjustment of the images is done to show what quality the results are.

ii) **Point cloud densification**- Here, the 3D point clouds will be generated based on the settings input by us. The triangle mesh will also be generated for the point clouds.

iii) **DSM, Orthomosaic and Index**- Here, the Digital Surface Model (DSM) and Orthomosaic (Stitching of the images together to form one image) will be generated.

After the processing, the polylines are drawn in the 3D point cloud in green colour to indicate the area of pavement distress. In the 3D point cloud of the project, polylines are drawn where the pavement distress are and in order to be accurate, the polylines drawn are edited in the image viewer in order to check that the polyline drawn is correct for each image which overlaps with the other. Also, a special feature about 3D point clouds is that it can be rotated so that polylines can be drawn where it is not visible from the top view. The length and area calculation of the pavement distress can also be generated using this software. The Orthomosaic and the polylines are exported for further use in AutoCAD Civil 3D 2015 software.

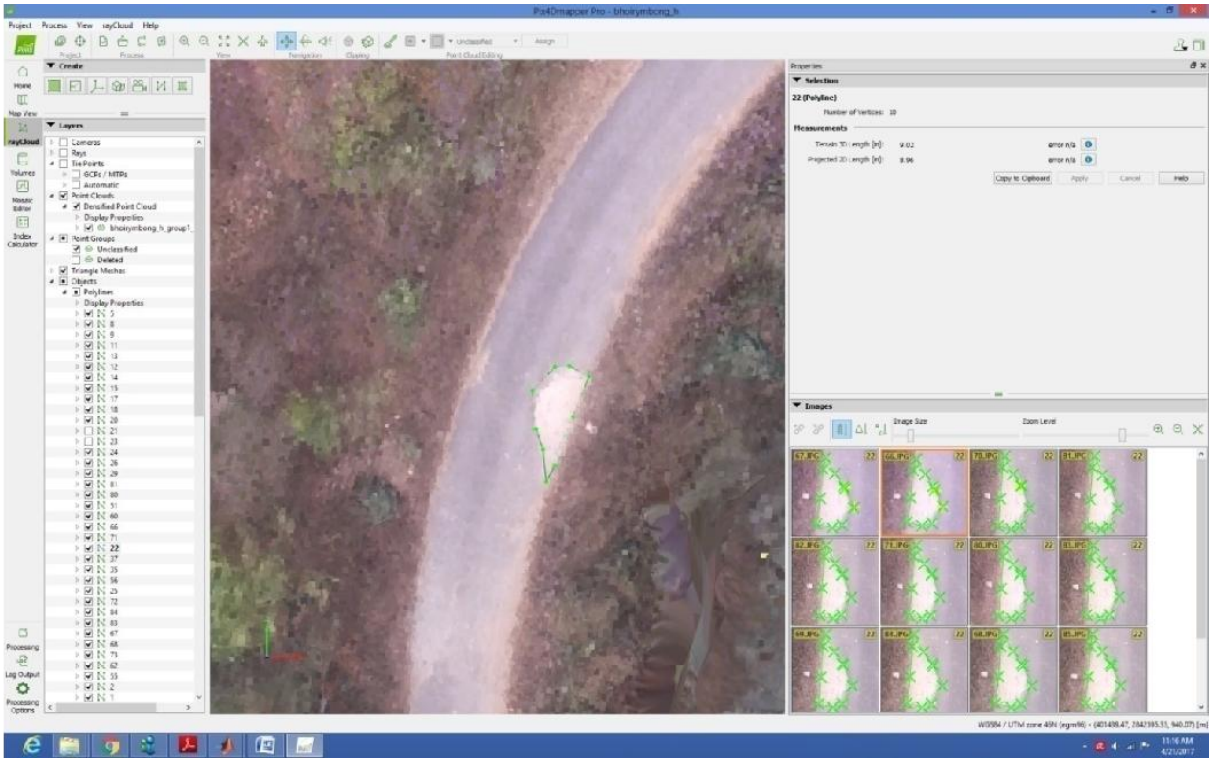

Figure 32: Creating the polylines in Pix4d software.

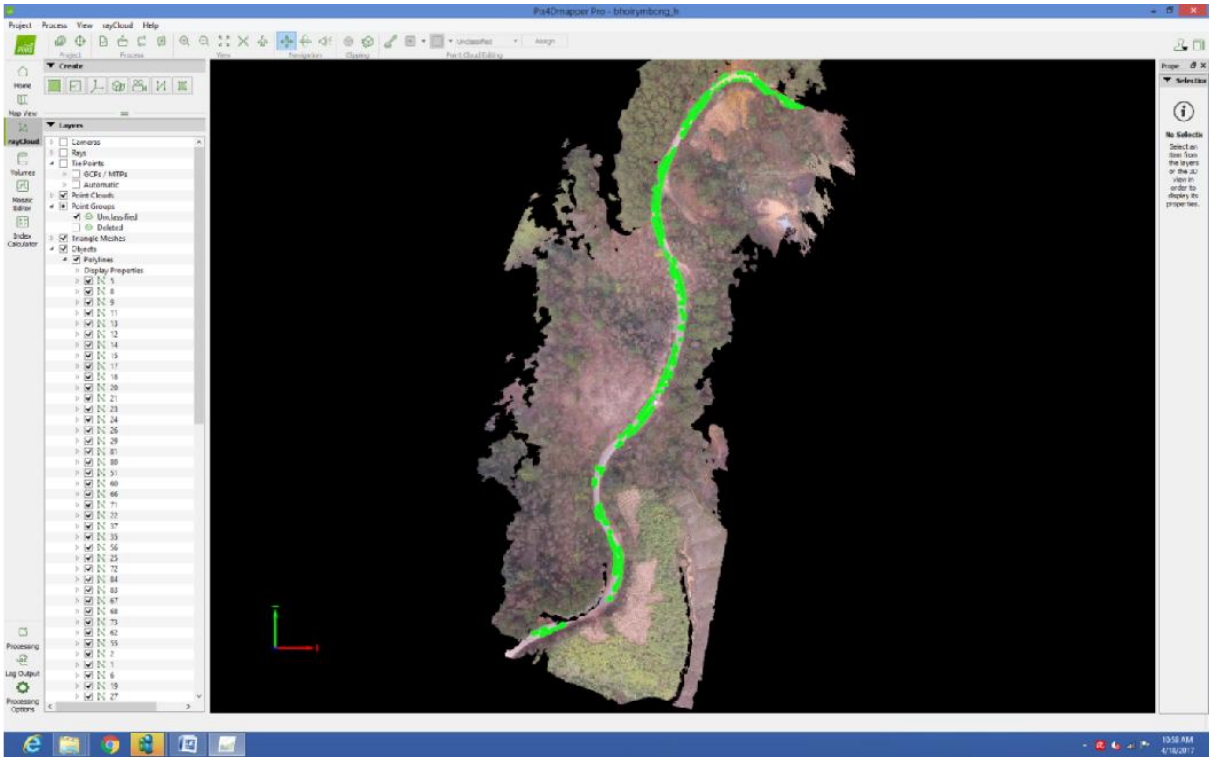

Figure 33: Site- Bhoirymbong. Top view of the point cloud in Pix 4D software.

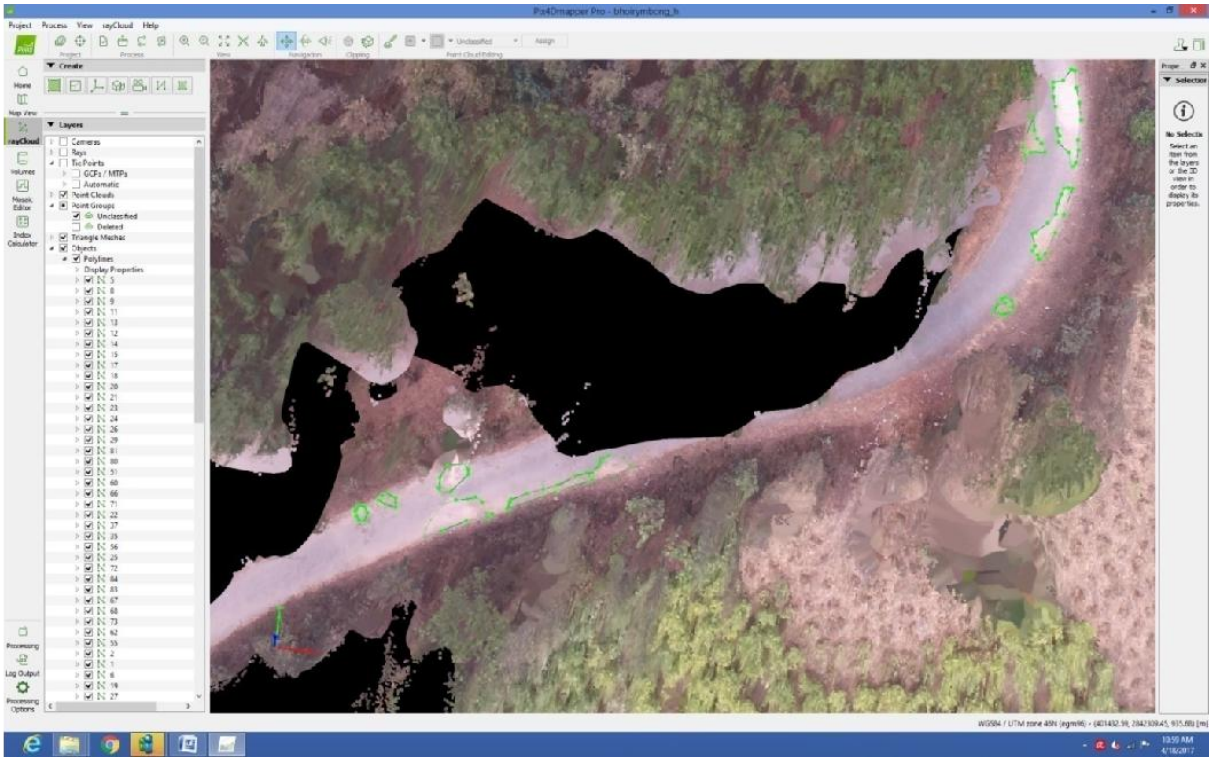

Figure 34: Site- Bhoirymbong. Due to the disturbance of trees, the road pavement is not visible in the point cloud.

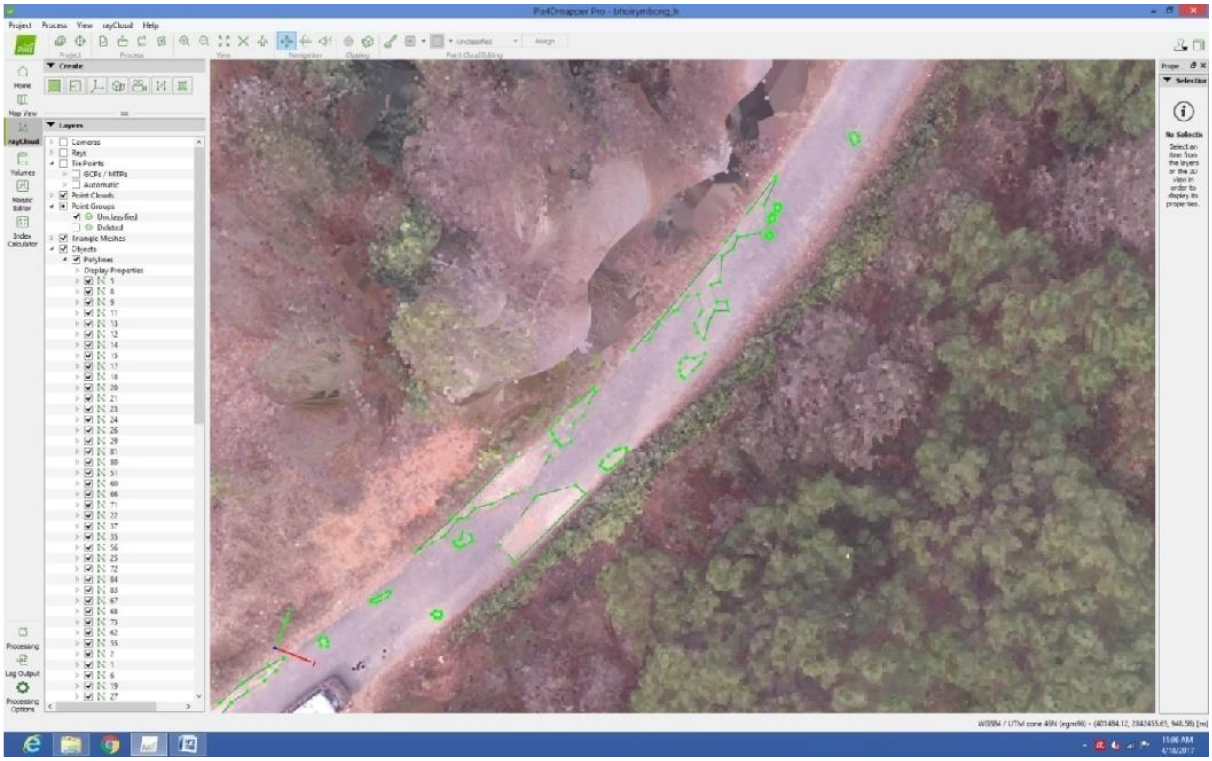

Figure 35: Site- Bhoirymbong. Part of the road segment where the pavement distresses can be identified in the point cloud in the form of polylines

.

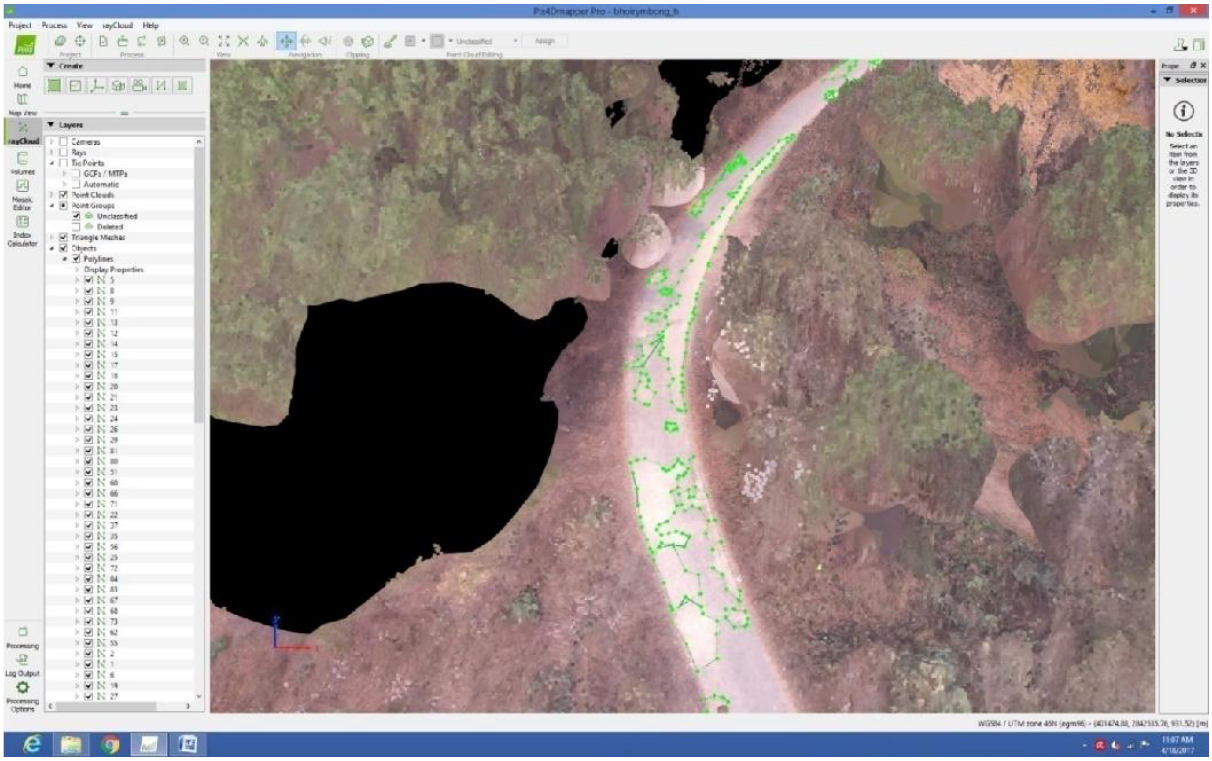

Figure 36: Site- Bhoirymbong. The point cloud is rotated for better visualization of the pavement.

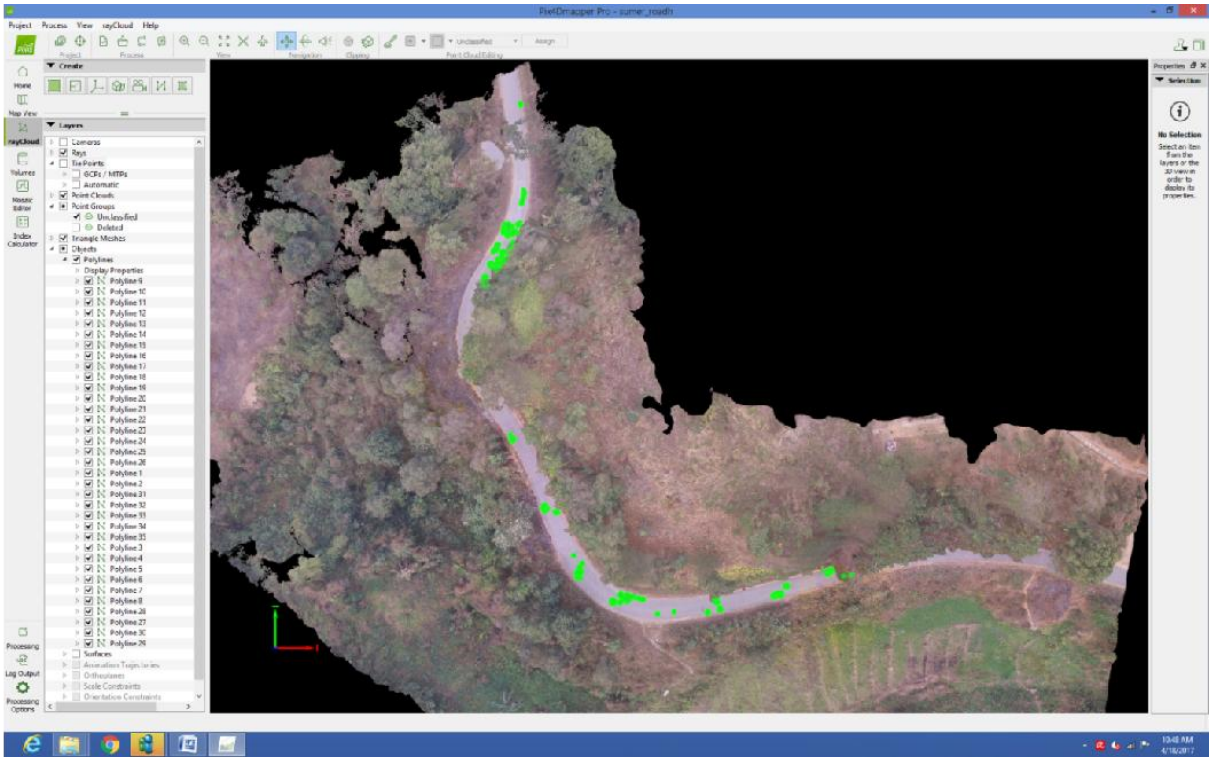

Figure 37: Site- Sumer 4 No. Top view of the point cloud in Pix 4D software.

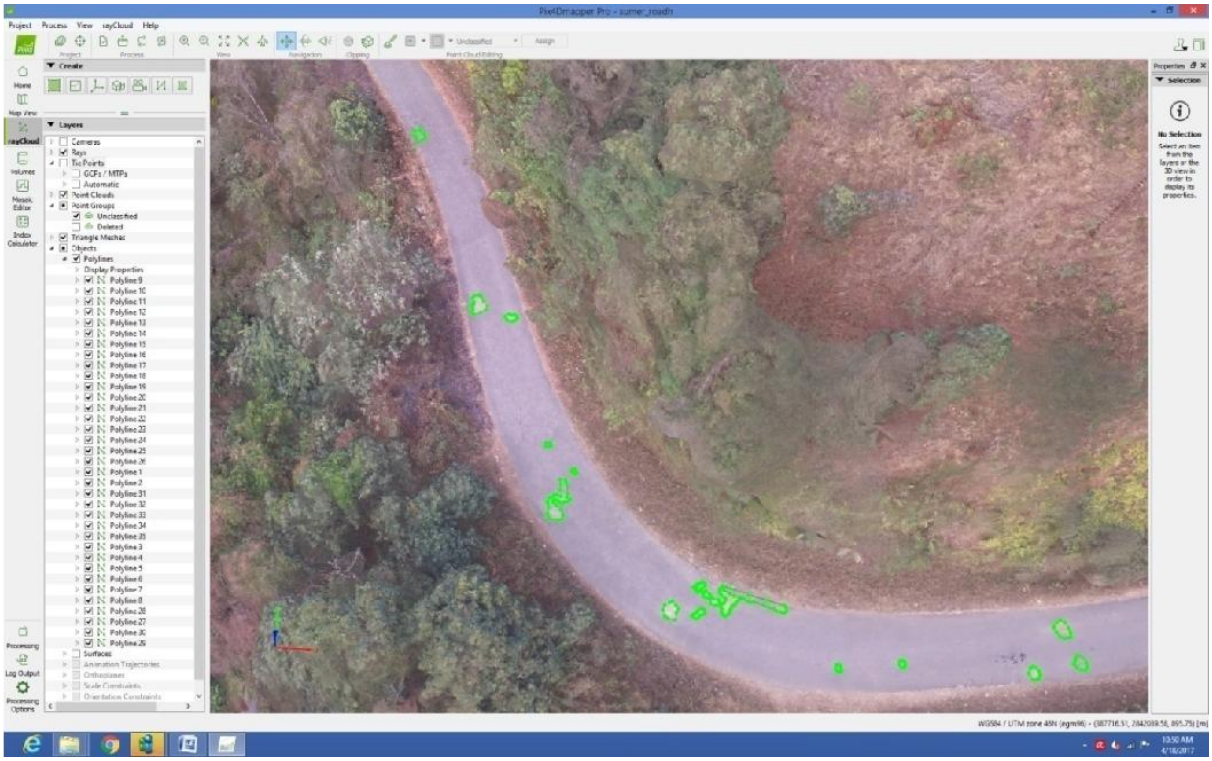

Figure 38: Site- Sumer 4 No. Part of the road segment where the pavement distresses can be identified in the point cloud in the form of polylines.

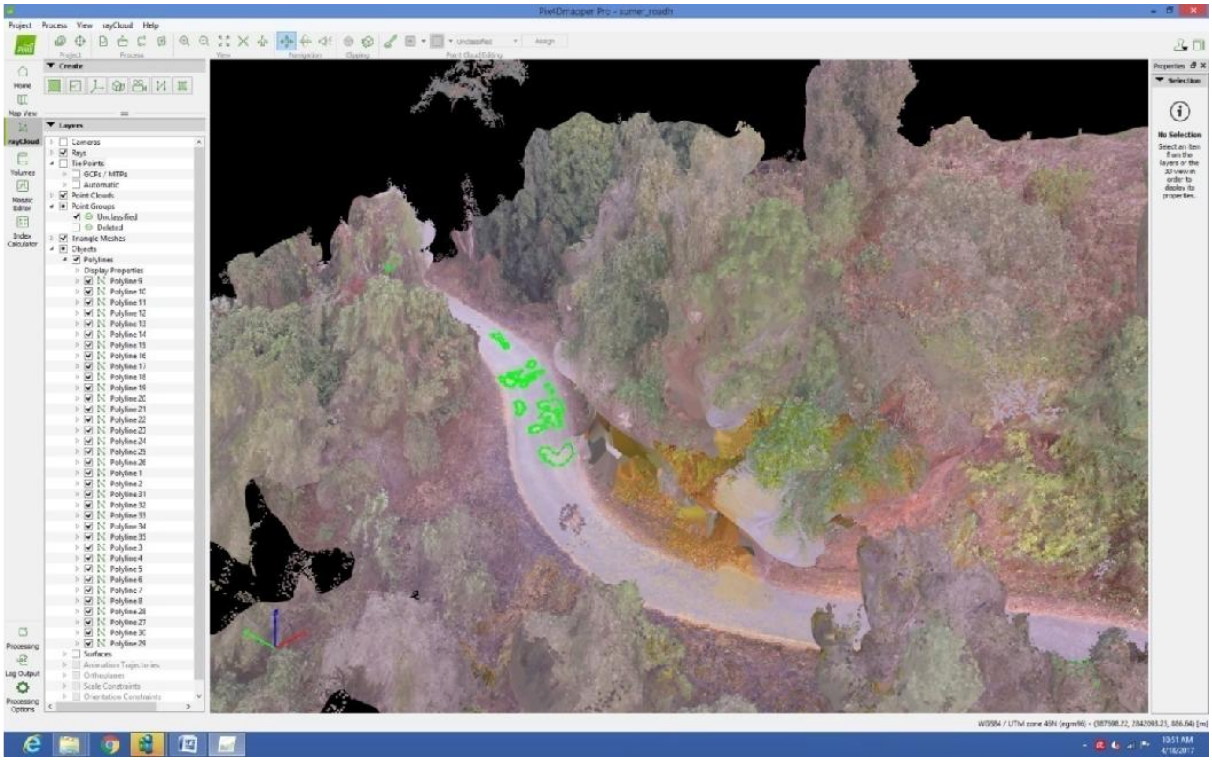

Figure 39: Site- Sumer 4 No. The point cloud is rotated for better visualization of the pavement.

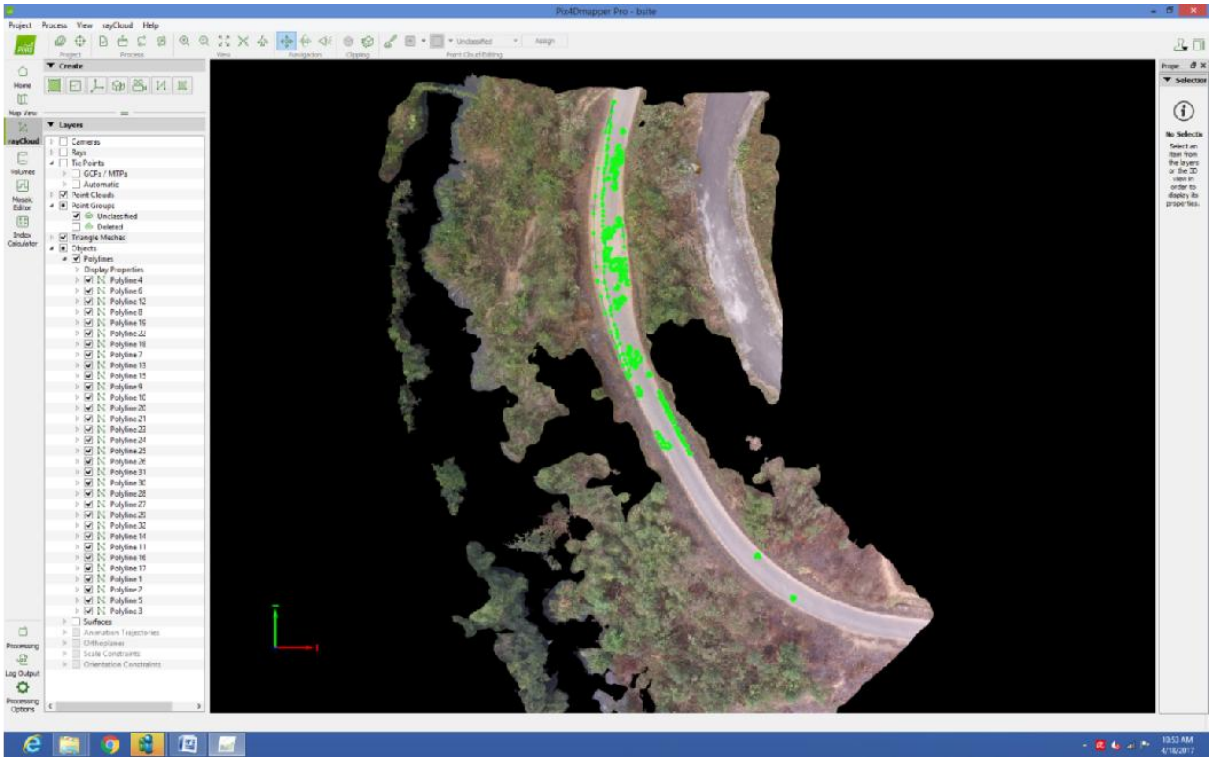

Figure 40: Site- Segment of the road in Umtham. Top view of the point cloud in Pix4d software.

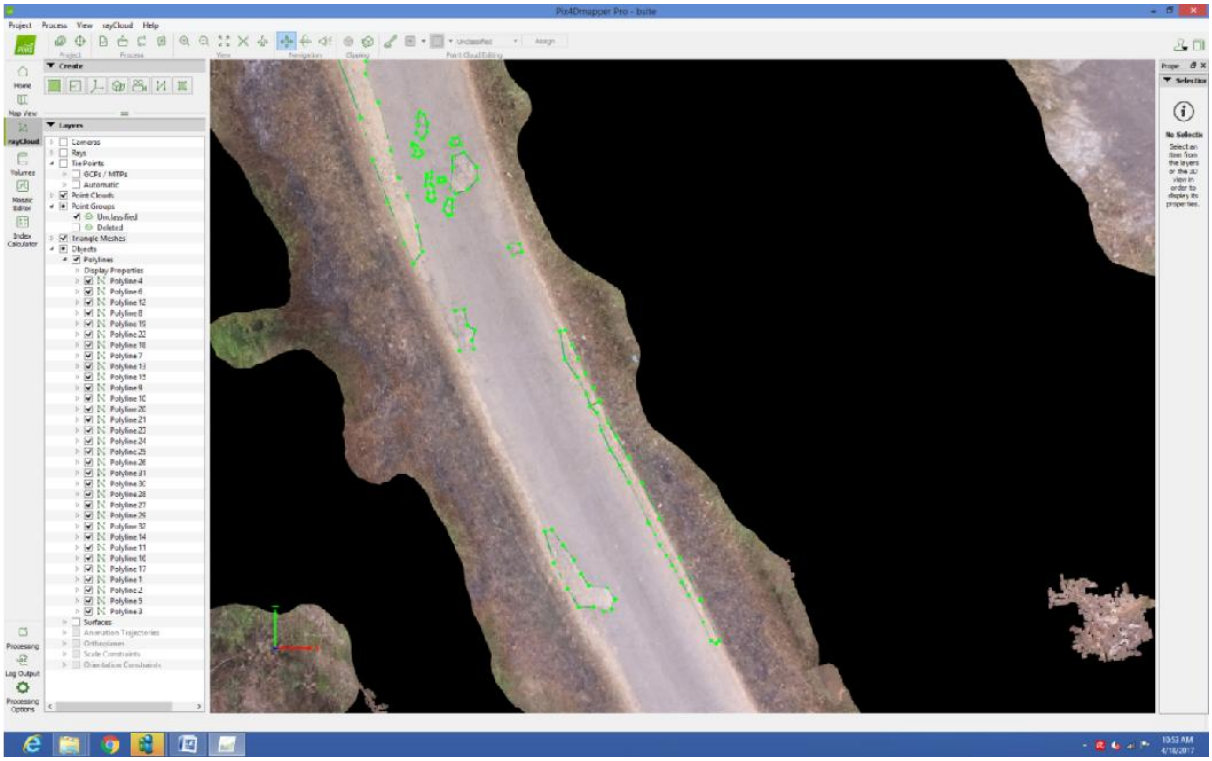

Figure 41: Site-Segment of the road in Umtham. Part of the road segment where the pavement distresses can be identified in the point cloud in the form of polylines.

The polylines are then exported as shape files which will be used as input to other software applications like AutoCAD Civil 3D.

4.6. MEASURING THE AREA OF PAVEMENT DISTRESS IN AUTOCAD CIVIL 3D

In AutoCAD Civil 3D 2015, the Orthomosaic is exported and polylines are drawn to show the pavement distresses and are measured. The polylines from Pix4d are exported to the Orthomosaic in order to add more information, in case the pavement distress were not clear in the Orthomosaic in AutoCAD and because the pavement distresses could not be all identified in the point cloud in Pix4d. The length of the road in Bhoirymbong is 450m (approx), Sumer 4 No is 250m (approx) and the segment of the road in Umtham is 120m (approx). This will act as a map to the Engineer or Surveyor in-charge denoting the pavement distresses along with the chainage of the road. These drawings or maps are given in **Appendix A**.

Table 9: Measurements of Bhoirymbong road.

Polyline	Pix4d Area(m^2)	AutoCAD Civil 3D Area (m^2)
1	0.625999	0.4
2	0.668684	0.63
3	2.61909	2.621
4	6.19551	6.071
5	5.72819	2.981
6	1.15145	1.184
7	5.91105	4.896
8	2.97631	3.46
9	3.21119	2.623
10	13.3456	12.203
11	3.84108	2.178
12	0.543087	0.557
13	5.0806	4.547
14	0.834985	0.718
15	0.84887	0.909
16	3.26212	3.317
17	1.78443	2.005
18	3.5755	not visible
19	0.75448	not visible
20	3.90537	4.379
21	3.44839	not visible
22	3.59619	3.559
23	0.75572	0.426
24	2.74496	2.281
25	7.90611	11.832
26	3.55412	2.918
27	1.9326	2.445
28	1.98456	8.756
29	9.41837	11.523
30	0.622551	
31	5.55699	
32	0.149265	0.133

33	0.200646	0.219
34	0.107498	0.482
35	6.24538	8.278
36	0.338308	
37	6.17994	not visible
38	2.13495	6.707
39	not generated	1.049
40	7.27757	3.507
41	0.775087	
42	0.080547	1.334
43	0.0944311	0.074
44	0.0842893	0.082
45	0.192327	0.937
46	1.18543	0.292
47	0.28378	0.224
48	1.62343	3.258
49	0.505204	0.516
50	0.39308	0.425
51	0.541623	3.657
52	4.53122	0.514
53	0.417605	0.192
54	0.440919	0.678
55	7.05618	6.515
56	17.0314	12.957
57	0.153387	not visible
58	0.0719488	not visible
59	0.322154	not visible
60	not generated	4.894
61	0.785892	0.784
62	4.44689	32.239
63	0.799306	
64	4.65573	
65	5.8433	
66	11.6768	

67	0.307681	0.371
68	43.3202	43.144
69	2.03063	0.971
70	5.22386	not visible
71	0.608435	0.669
72	0.422938	0.621
73	1.39066	not visible
74	0.284782	0.414
75	2.42479	not visible
76	0.779423	not visible
77	0.171694	0.194
78	5.9691	7.253
79	not generated	10.052
80	23.2425	145.89
81	12.0982	
82	4.82413	
83	126.049	
84	35.8588	8.954
A	not visible	1.013
B	not visible	0.198
C	not visible	1.111
D	not visible	0.134
E	not visible	0.18
F	not visible	0.275
G	not visible	1.038
H	not visible	0.306
I	not visible	2.316
J	not visible	0.022
K	not visible	1.804
L	not visible	0.661
M	not visible	0.07
N	not visible	0.018
O	not visible	0.119
P	not visible	0.586

Q	not visible	0.34
R	not visible	0.095
S	not visible	0.306
T	not visible	0.429
U	not visible	0.162
V	not visible	0.031
W	not visible	0.279
X	not visible	2.576

Table 10: Measurements of Sumer 4 No road.

Polyline	Pix4d Area(m^2)	AutoCAD Civil 3D Area (m^2)
1	0.169247	0.078
2	1.24411	1.314
3	0.547206	0.851
4	2.37598	2.307
5	0.688701	0.735
6	0.137154	0.139
7	0.490277	0.409
8	0.096167	0.11
9	not generated	0.129
10	1.18232	0.861
11	4.89765	5.337
12	1.09807	1.696
13	2.80648	3.328
14	0.960903	0.895
15	1.23316	1.454
16	0.407251	0.381
17	0.08532	0.09
18	0.077885	0.13
19	1.70007	2.092
20	0.660563	0.769
21	0.232819	0.351
22	0.219448	0.214

23	0.310654	0.341
24	0.937227	3.37
25	1.35241	
26	0.096358	0.085
27	0.095489	0.111
28	0.314414	0.282
29	0.63947	0.667
30	0.442612	0.374
31	1.93393	1.77
32	0.413592	0.345
33	1.44629	not visible
34	0.196435	0.201
35	0.243834	0.283
A	not visible	0.742
B	not visible	0.188
C	not visible	0.306
D	not visible	0.058
E	not visible	0.314
F	not visible	0.048
G	not visible	3.918
H	not visible	0.154

Cracks are also present in the pavement surface. The length of each crack is not measured but the whole road length and width of the pavement surface where the cracks are present are measured.

Road length = 39.7891 m

Road width = 3.80 m (approx)

Table 11: Measurements of a segment of a road in Umtham.

Polyline	Pix4d Area(m^2)	AutoCAD Civil 3D Area (m^2)
1	0.167422	0.224
2	0.299857	0.211
3	2.97419	1.056
4	0.883843	not visible

5	2.04904	2.039
6	0.63647	53.065
7	0.14092	
8	50.1277	
9	0.124677	
10	0.193413	
11	0.0330107	0.194
12	0.983815	0.205
13	0.0690432	0.161
14	0.0907383	1.007
15	0.252423	
16	0.467116	0.187
17	0.502737	0.065
18	0.149863	0.22
19	17.0438	0.351
20	0.483476	0.561
21	0.0752219	0.144
22	1.6368	0.302
23	1.05077	0.402
24	0.209032	0.329
25	not generated	1.624
26	0.124006	0.164
27	0.220951	0.235
28	1.24585	3.019
29	0.221295	
30	not generated	
31	0.582339	0.229
32	0.190472	0.197

CHAPTER 5

CONCLUSION

5.1 CONCLUSION

The proposed solution by using UAV for road maintenance purposes is effective and pavement defects like cracks, depression, potholes, ravelling, shoving, corrugation and unpaved surface could be processed and analyzed resulting in overall Precision of 96.57%, Recall of 75.80% and Tracking Accuracy of 74.13%. The data collected with the help of UAV can also be used as an Inventory data for further planning and decision making purposes. The proposed method will serve as a means to collect information in order to provide an Information System for Engineers or Surveyors. Areas which are inaccessible to man either by vehicle or foot can be accessed with the help of UAV. This will help to manage the cost and time and will help to complete the road maintenance work as and when required. Some of the pavement defects could not be analyzed, hence further research work and development of UAV is essential. However, the use of UAV seems promising and advantageous to engineers and as well in the future.

Table 12: Comparison of the conventional method and the proposed method

<table>
<tr><th></th><th colspan="2">CONVENTIONAL METHOD</th><th>PROPOSED METHOD (UAV)</th></tr>
<tr><th>ACTIVITY</th><th>Recommended Task Rate</th><th>Remark</th><td rowspan="2"></td></tr>
<tr><td rowspan="2">Inspection of road</td><td>20 km/wd</td><td>Inspection by vehicle</td><td rowspan="2">1 km could be inspected in less than 30 minutes</td></tr>
<tr><td>10 km/wd</td><td>Inspection by foot</td></tr>
<tr><td>Monitoring Cost</td><td colspan="2">More cost is incurred as it involves more staff and time.</td><td>Less cost is incurred due to its flexibility and manoeuvrability</td></tr>
<tr><td>Pavement defects detection</td><td colspan="2">Since it is done manually, the pavement defects can all be noted</td><td>Since the UAV is flown at an altitude, the lower the altitude better is the resolution and the pavement defects can be recorded in the form of images or videos</td></tr>
</table>

Severity defects detection	More time is needed	Lesser time needed
Severity Analysis	Different severity levels exists for each defect, usually, Low, Medium and High	The security level is categorised as highest to lowest for all the pavement defects
Measurement of the pavement distress	It is done by a long ruler and tape and is time consuming	Due to the geo-referenced properties of the Orthomosaic obtain from Pix4d, measurements can be done by drawing polylines around the pavement distress area
Defects counting for assessment	Yes, but is time consuming	Yes, but is time saving
Area coverage with respect to time	More time is needed especially if the area is inaccessible	Can finish a large area in a lesser time
Inventory Data	Not reliable as the data is not updated	Reliable due to its real time monitoring capabilities
Disaster response	Human labour is required so it is risky	It can aid where it is not possible to man
Safety	Areas which are inaccessible and risky makes safety a concern	It can fly to areas where safety is a concern

5.2. LIMITATIONS OF THE STUDY

The difficulties faced during the study are as follows:

i) Tree and wire disturbances. Hence, proper altitude could not be maintained.

ii) Poor flight planning, hence poor images.

iii) Disturbances in the roads like cars, pedestrians, etc.

iv) If there is less overlapping of the images, the Orthomosaic image generated in software for UAV like Pix4d will not be clear.

v) In the study area, autonomous flying seems risky and manual flying had to be conducted.

vi) If there are much garbage like plastics, leaves, etc. and if the UAV images contain shadow on the pavement surface then, while processing, it interferes with the results.

5.3. FUTURE SCOPE

UAV technology is emerging and developing and its applications are widely used for civil activities. The following are the future scope for developing the UAV applications for road monitoring purposes:

i) The UAV used for collecting the data needs to be improved as well as the sensors associated with it.

ii) Automatic processing of the images having pavement defects will improve rather than manual processing. This automatic processing should be done by the UAV itself so that the data will automatically be generated along with the images or videos.

iii) Some of the pavement defects cannot be visualized nicely and hence further research to improve the algorithm is needed.

iv) Pix4d software, which is an emerging technology, should develop for road monitoring purposes.

v) The data is in 2D format, so if the data is made available in 3D format, it will improve the scenario of road monitoring as the volume can also be calculated.

REFERENCES

1. Ahmed, M., Haas, C.T., and Haas, R., (2011), "Toward low-cost 3D automatic pavement distress surveying: the close range photogrammetry approach", Canadian Journal of Civil Engineering, Vol. No- 38, pp. 1301–1313.
2. Adlinge, S. S., and Gupta, A. K., (2013), "Pavement Deterioration and its Causes", Journal of Mechanical & Civil Engineering (IOSR-JMCE), ISSN: 2278-1684, pp. 09-15.
3. Anca, P., Calugaru, A., Alixandroae, I., and Nazarie, R., (2016), "A Workflow For UAV's Integration Into A Geodesign Platform", The International Archives of the Photogrammetry, Remote Sensing and Spatial Information Sciences, XXIII ISPRS Congress, Volume XLI-B1, pp. 1099- 1103.
4. Articles about Orthomosaic and Photo stitching in Pix4d software.
5. Buchinger, D., and Silva, A.G., (2014), "Anomalies detection in asphalt pavements: a morphological image processing approach", Revista Brasileira de Computação Aplicada (ISSN 2176-6649), Passo Fundo, Vol. 6, No. 1, pp. 121-129.
6. Branco, L.H.C., and Segantine, P.C.L., (2015), "MaNIAC-UAV - A methodology for automatic pavement defects detection using images obtained by Unmanned Aerial Vehicles", 4th International Conference on Mathematical Modeling in Physical Sciences (IC-MSquare2015) IOP Publishing, Journal of Physics: Conference Series633, 012122.
7. Barry, P., (2016), "Point clouds, not dust clouds – the benefits of drones to society", Engineers Journal.
8. Chou, E.Y., and Salari, E., (2010), "A Novel Image Database Analysis System for Maintenance of Transportation Facility – Phase I", The University of Toledo – University Transportation Center, Project Number: UTUTC-IU-5.
9. Colomina, I., and Molina, P., (2014), "Unmanned aerial systems for photogrammetry and remote sensing: A review", ISPRS Journal of Photogrammetry and Remote Sensing, Vol. 92, pp. 79–97.
10. Chikhradze, N., Henriques, R., Elashvili, M., Kirkitadze, G., Janelidze, Z., Bolashvili, N., Lominadze, G., (2015), "Close Range Photogrammetry in the Survey

of the Coastal Area Geoecological Conditions (on the Example of Portugal)", Earth Sciences, 4(5-1), pp. 35-40.

11. Costa, D.B., Melo, R.R.S.de., Alvares, J.S., and Bello, A.A., (2016), "Evaluating the Performance of Unmanned Aerial Vehicles for Safety Inspection", Proceedings of 24th Annual Conference of the International Group for Lean Construction, pp. 23-32.
12. Eisenbeiss, H., (2004), "A Mini Unmanned Aerial Vehicle (UAV): System Overview and Image Acquisition", International Workshop on Processing and Visualization Using High-Resolution Imagery, 18-20 November, Pitsanulok, Thailand.
13. Eschmann, C., Kuo, C.M., Kuo, C.H., and Boller, C., (2012), "Unmanned Aircraft Systems for Remote Building Inspection and Monitoring", 6th European Workshop on Structural Health Monitoring, Th.2.B.1.
14. Example files for "Image Processing Made Easy" Webinar, by Andy Thé, 2016.
15. Fendi, K.G., Adam, S. M., Kokkas, N., and Smith, M., (2014), "An Approach to Produce a GIS Database for Road Surface Monitoring", Asia-Pacific Chemical, Biological & Environmental Engineering Society (APCBEE), pp. 235-240.
16. Furbas, S., (2015), "UAV pavement inspections", Article, airsightNextGen Airfield Inspections.
17. Gopi, S., (2007), "Advanced Surveying: Total Station, GIS and Remote Sensing", Book, Pearson Education India.
18. Ghanta, S., Birken, R., and Dy, J., (2012), "Automatic Road Surface Defect Detection from Grayscale Images", Proceedings of Society of Photographic Instrumentation Engineers, Vol. 8347, 83471E.
19. Grandsaert, P.J., (2015), "Integrating Pavement Crack Detection And Analysis Using Autonomous Unmanned Aerial Vehicle Imagery", Thesis, Air Force Institute of Technology, Ohio.
20. Gupta, C., Chutia, D., Kithan, M., Kesiezie, A-O., Saikhom, V., Singh, P.S., Chouhan, A., Sharma, N., Debnath, A., Handique, B.K., Goswami, J., Goswami, C., Khan, A.Q., Sarma, K.K., and Raju, P.L.N., (2016), "Design and Integration of a Lightweight Multirotor Unmanned Aerial Vehicle for Remote Sensing Applications", Asian Association on Remote Sensing.
21. Hunt, B.R., Lipsman, R.L., Rosenberg, J.M., with Coombes, K.R., Osborn, J.E., and Stuck, G.J., (2001), "A Guide to MATLAB for Beginners and Experienced Users", Book, Cambridge University Press.

22. Horcher, A., and Visser, R.J.M., (2004), "Unmanned Aerial Vehicles: Applications for Natural Resource Management and Monitoring", Council on Forest Engineering (COFE), Conference Proceedings: “Machines and People, The Interface”, Hot Springs, April 27-30.
23. Hart, W.S., and Gharaibeh, N.G., (2010), "Use Of Micro Unmanned Aerial Vehicles for Roadside Condition Assessment", Technical Report, Texas Transportation Institute, Report no- SWUTC/10/476660-00019-1.
24. Ham, Y., Han, K. K., Lin, J. J., and Golparvar-Fard, M., (2016), "Visual monitoring of civil infrastructure systems via camera-equipped Unmanned Aerial Vehicles (UAVs): a review of related works", Visualization in Engineering, 4:1.
25. Irizarry, J., Gheisari, M., and Walker, B.N., (2012), "Usability Assessment of Drone Technology as Safety Inspection Tools", Journal of Information Technology in Construction, ISSN 1874-4753, Vol no.17, pp. 194-212.
26. Jing, L., and Aiqin, Z., (2010), "Pavement Crack Distress Detection Based on Image Analysis", International Conference on Machine Vision and Human-machine Interface, pp. 576-579.
27. Jog, G. M., Koch, C., Golparvar-Fard, M., and Brilakis, I., (2012), “Pothole Properties Measurement through Visual 2D Recognition and 3D Reconstruction”, International Conference on Computing in Civil Engineering.
28. Koch, C., and Brilakis, I., (2011), “Pothole Detection in Asphalt Pavement Images”, Advanced Engineering Informatics, Vol. 25, Issue. 3, pp. 507-515.
29. Koch, C., Jog, G.M., and Brilakis, I, (2013), "Automated Pothole Distress Assessment Using Asphalt Pavement Video Data", Journal of Computing in Civil Engineering.
30. Karantzalos, K., Koutsourakis, P., Kalisperakis, I., Grammatikopoulos L., (2015), "Model-Based Building Detection From Low-Cost Optical Sensors Onboard Unmanned Aerial Vehicles", The International Archives of the Photogrammetry, Remote Sensing and Spatial Information Sciences, International Conference on Unmanned Aerial Vehicles in Geomatics, Volume XL-1/W4, pp. 293- 297.
31. Kim, J,W., Kim, S,B., Park, J,C., and Nam, J,W., (2015), “Development of Crack Detection System with Unmanned Aerial Vehicles and Digital Image Processing” , Advances in Structural Engineering and Mechanics (ASEM15), pp. 25-29.

32. Kumar, R., and Parida, P., (2016), "Application of Geospatial Technology in Effective Planning of PMGSY", A National Conference on Fifteen Years of PMGSY (FYPMGSY), Transportation Engineering Group, Civil Engineering Department, Indian Institute of Technology Roorkee,Roorkee-247667 (Uttarakhand), August 6-7.
33. Khatri, A., (2016), "Maintenance Free Planning Of A Transportation System- An Image Processing Approach", 9th Urban Mobility India Conference and Expo.
34. Liu, P., Chen, A.Y., Huang, Y.N., Han, J.Y., Lai, J.S., Kang, S.C., Wu, T.H., Wen, M.C., and Tsai, M.H., (2014), "A review of rotorcraft Unmanned Aerial Vehicle (UAV) developments and applications in civil engineering ", Smart Structures and Systems, Vol. 13, No. 6, pp. 1065-1094.
35. Multi ROI/Mask Editor Class, by Jonas Reber, 2011 from MATLAB File Exchange.
36. Mohammed, F., Idries, A., Mohamed, N., Al-Jaroodi, J., and Jawhar, I., (2014), "UAVs for Smart Cities: Opportunities and Challenges", International Conference on Unmanned Aircraft Systems (ICUAS), May 27-30, pp. 267-273.
37. Managing Maintenance of Rural Roads in India, National Rural Roads Development Agency, Ministry of Rural Development, Government of India, 2014.
38. Maurice, M.J., Koeva, M.N., Gerke, M.,Nex, F., Gevaert, C., (2015), "A photogrammetric approach for map updating using UAV in Rwanda", Geo Tech Rwanda, Kigali, 18-20 November.
39. Mandal, M., Katageri, M., Gandhi, M., Koregaonkar, N., and Sengupta, S., (2015), "Automated Management Of Pothole Related Disasters Using Image Processing and Geotagging", International Journal of Computer Science & Information Technology (IJCSIT), Vol 7, No 6, pp. 97-106.
40. Nienaber, S., Booysen, M.J., and Kroon, R.S., (2015), "Detecting Potholes Using Simple Image Processing Techniques And Real-World Footage", Southern African Transport Conference (SATC).
41. NHAI signs MoU with ISRO and NECTAR for use of spatial technology for monitoring and managing National Highways, Press Information Bureau, Government of India, Ministry of Road Transport & Highways, 13-January-2016, Accessed 8 May 2016.
42. Pavement Distress Identification Manual for the NPS Road Inventory Program prepared by Federal Highway Administration, Department of Transportation, United States of America, 2006-2009.

43. Prathiba, T.,Thamaraiselvi, M., Mohanasundari, M., and Veerelakshmi, R., (2015), "Pothole Detection In Road Using Image Processing", BEST: International Journal of Management, Information Technology and Engineering (BEST: IJMITE), ISSN 2348-0513, Vol. 3, Issue 4, pp. 13-20.
44. Pan, Y., Zhang, X., Jin, X., Yu, H.,Rao, J.,Tian, S.,Luo, L., and Li, C., (2016), "Road pavement condition mapping and assessment using remote sensing data based on MESMA", 9th Symposium of the International Society for Digital Earth (ISDE), OP Conference Series: Earth and Environmental Science, Vol No.34.
45. Rajab, M.I., Alawi, M.H., and Saif, M.A., (2008), "Application of Image Processing to Measure Road Distresses", WSEAS Transactions on Information Science & Applications, Issue 1, Volume 5.
46. Ryu, S.K., Kim, T., and Kim, Y. R., (2015), "Image-Based Pothole Detection System for ITS Service and Road Management System", Mathematical Problems in Engineering, Article ID 968361, 10 pages.
47. Radopoulou, S,C., and Brilakis, I., (2015), "Patch detection for pavement assessment", Automation in Construction, 53, pp. 95–104.
48. Rural Road Maintenance training modules for field engineers, Ministry of Rural Development, Government of India, October 2015.
49. Sun, Y., (2009), "Automated Pavement Distress Detection Using Advanced Image Processing Techniques", Thesis, The University of Toledo.
50. Salari, E., and Bao, G., (2011), "Pavement Distress Detection and Severity Analysis", Proceedings of Society of Photographic Instrumentation Engineers-IS&T, Vol. 7877, 78770C.
51. Samad, A.M., Kamarulzaman, N., Hamdani, M.A., Mastor, T.A., and Hashim, K.A., (2013), "The Potential of Unmanned Aerial Vehicle (UAV) for Civilian Mapping and Application", IEEE 3rd International Conference on System Engineering and Technology, pp. 313-318.
52. Siebert, S., and Teizer, J., (2014), "Mobile 3D mapping for surveying earthwork projects using an Unmanned Aerial Vehicle (UAV) system", Automation in Construction, Vol. No.14, pp. 1-14.
53. Sankarasrinivasan, S., Balasubramanian, E., Karthik, K., Chandrasekar, U., and Gupta, R., (2015), "Health Monitoring of Civil Structures with Integrated UAV and

Image Processing System", Proceedings of 11th International Multi-Conference on Information Processing, pp. 508-515.

54. Schnebele, E., Tanyu, B. F., Cervone, G., and Waters, N., (2015), "Review of remote sensing methodologies for pavement management and assessment", European Transport Research Review, 7:7.
55. Tiong, P.L.Y., Mustaffar, M., and Hainin, M.R., (2012), "Road Surface Assessment of Pothole Severity by Close Range Digital Photogrammetry Method", World Applied Sciences Journal 19 (6),pp. 867-873.
56. Vacanas, Y., Themistocleous, K., Agapiou, A., and Hadjimitsis, D., (2015), "Building Information Modelling (BIM) and Unmanned Aerial Vehicle (UAV) technologies in infrastructure construction project management and delay and disruption analysis ", Third International Conference on Remote Sensing and Geo-information of the Environment, Vol. 9535, 95350C, pp. 1-11.
57. Yang, C.H., Wen, M.C., Chen, Y.C., and Kang, S.C., (2015), "An Optimized Unmanned Aerial System for Bridge Inspection", International Symposium on Automation and Robotics in Construction and Mining.
58. Younkin, K., (2015), "Use of UAVs on heavy/civil construction and public infrastructure", Research Proposal, Iowa State University.
59. Zhang, C., (2008), "An UAV-Based Photogrammetric Mapping System For Road Condition Assessment", The International Archives of the Photogrammetry, Remote Sensing and Spatial Information Sciences, Vol. XXXVII, Part B5, Beijing.

APPENDIX A

APPENDIX B

MATLAB Code 1

This Code is for cracks.

```
%% load image
[filename, pathname, filterindex] = uigetfile( ...
{  '*.jpg','JPEG (*.jpg)'; ...
   '*.bmp','Windows Bitmap (*.bmp)'; ...
   '*.fig','Figures (*.fig)'; ...
   '*.*',  'All Files (*.*)'}, ...
   'Choose image(s) to be processed', ...
   'MultiSelect', 'off');
iffilterindex==0,break;end
filename=cellstr(filename);
Im= imread(horzcat(pathname,char(filename)));
%% Solution:  Thresholding the image on each color pane
I=Im;
rmat=Im(:,:,1);
gmat=Im(:,:,2);
bmat=Im(:,:,3);
figure,imshow(I)
title('Original Image');
%% Image adjust
Istrech = imadjust(I,stretchlim(I));
figure,imshow(Istrech)
title('Contrast stretched image')
%% Convert RGB image to gray
Igray_s = rgb2gray(Istrech);
figure,imshow(Igray_s,[])
title('RGB to gray (contrast stretched) ')
%% Image segmentation by thresholding
level = 0.68;
Ithres = im2bw(Igray_s,level);
figure,imshow(Ithres)
title('Segmented cracks')
```

```
%%
K=medfilt2(Ithres);
figure, imshow(K);
title('Median Filtered Image')
%% Image morphological operation
BW2 = bwmorph(K,'clean',1);
figure,imshow(BW2)
title('Cleaned image')
%%
se=strel('disk',1);
closeBW = imclose(BW2,se);
figure, imshow(closeBW);
title('Closed Image')
```

MATLAB Code 2

This code is for potholes, etc.

```
%% load image
clear all;
close all;
[filename, pathname, filterindex] = uigetfile( ...
{  '*.jpg','JPEG (*.jpg)'; ...
   '*.bmp','Windows Bitmap (*.bmp)'; ...
   '*.fig','Figures (*.fig)'; ...
   '*.*',  'All Files (*.*)'}, ...
   'Choose image(s) to be processed', ...
   'MultiSelect', 'off');
iffilterindex==0, break;end
filename=cellstr(filename);
I= imread(horzcat(pathname,char(filename)));
figure,imshow(I);
title('Original Image');
%% Image adjust
Istrech = imadjust(I,stretchlim(I));
figure,imshow(Istrech)
title('Contrast stretched image')
%% Convert RGB image to gray
Igray_s = rgb2gray(Istrech);
figure,
imshow(Igray_s,[])
title('RGB to gray (contrast stretched) ')
%% Image segmentation by thresholding
level = 0.69;
Ithres = im2bw(I,level);
figure,imshow(Ithres)
title('Segmented cracks')
 %Image morphological operation
BW2 = bwmorph(Ithres,'clean',1);
%figure,
imshow(BW2)
%title('Cleaned image')
```

```
BW2 = bwmorph(Ithres,'thin', inf);
%figure,
imshow(BW2)
title('Thinned image')
BW2 = imfill(Ithres, 'holes');
figure,imshow(BW2)
title('Filled image')
```

MATLAB Code 3

This code was originally coded by Jonas Reber on 6th May 2011. However, some modifications were made. This is for defining the Region of Interest or Mask.

```
classdef CROIEditor2 < handle
    %%
events
MaskDefined  % to get the ROI information (obj.getROIData)
end
properties
image    % image to work on, obj.image = theImageToWorkOn
roi      % the generated ROI mask (logical)
labels   % Connected component labens (multi ROI)
number   % how many ROIs there are
figh = 300; % initial figure height - your image is scaled to fit.
end
properties(Access=private)
        % UI stuff
guifig    % mainwindow
imax    % holds working area
roiax   % holds roid preview image
imag    % image to work on
roifig  %roi image
tl      % userinfo bar
figw      % initial window height, this is calculated on load
hwar = 2.1;  % aspect ratio
        % Class stuff
loadmask  % mask loaded from file
mask      % mask defined by shapes
current      %  which shape is selected
shapes = {}; % holds all the shapes to define the mask
        % load/save information
filename
pathname
end
    %% Public Methods
methods
```

```
function this = CROIEditor2(theImage)
        % constructor
this.figw = this.figh*this.hwar;
            % invoke the UI window
this.createWindow;
            % load the image
ifnargin> 0
this.image = theImage;
else
this.image = ones(200,200);
end
            % predefine class variables
this.current = 1;
this.shapes = {}; % no shapes at start
this.filename = 'mymask'; % default filename
this.pathname = pwd;      % current directory
end
function delete(this)
        % destructor
delete(this.guifig);
end
functionset.image(this,theImage)
        % set method for image. uses grayscale images for region
selection
if size(theImage,3) == 3
this.image = im2double(rgb2gray(theImage));
elseif size(theImage,3) == 1
this.image = im2double(theImage);
else
error('Unknown Image size?');
end
this.resetImages;
this.resizeWindow;
end
functionset.figh(this,height)
this.figh = height;
this.figw = this.figh*this.hwar;
this.resizeWindow;
```

```
end
function [roi, labels, number] = getROIData(this,varargin)
        % retrieve ROI Data
roi = this.roi;
labels = this.labels;
number = this.number;
end
end
    %% private used methods
methods(Access=private)
        % general functions ----------------------------------------
------
functionresetImages(this)
this.newROI;
            % load images
this.imag = imshow(this.image,'parent',this.imax);
this.roifig = imshow(this.image,'parent',this.roiax);
            % set masks to blank
this.loadmask = zeros(size(this.image));
end
functionupdateROI(this, a)
set(this.tl,'String','ROI not
saved/applied','Visible','on','BackgroundColor',[255 182 193]./256);
this.mask = this.loadmask | zeros(size(this.image)) ;
fori=1:numel(this.shapes)
BWadd = this.shapes{i}.createMask(this.imag);
this.mask = this.mask | BWadd;
end
set(this.roifig,'CData',this.image.*this.mask);
end
functionnewShapeCreated(this)
set(this.shapes{end},'Tag',sprintf('imsel_%.f',numel(this.shapes)));
this.shapes{end}.addNewPositionCallback(@this.updateROI);
this.updateROI;
end
       % CALLBACK FUNCTIONS
       % window/figure
functionwinpressed(this,h,e,type)
```

```
SelObj = get(gco,'Parent');
            Tag = get(SelObj,'Tag');
if and(~isempty(SelObj),strfind(Tag,'imsel_'))
this.current = str2double(regexp(Tag,'\d','match'));
fori=1:numel(this.shapes)
ifi==this.current
setColor(this.shapes{i},'red');
else
setColor(this.shapes{i},'blue');
end
end
end
end
functionclosefig(this,h,e)
delete(this);
end;
        % button callbacks ----------------------------------------
------
functionpolyclick(this, h,e)
this.shapes{end+1} = impoly(this.imax);
this.newShapeCreated; % add tag, and callback to new shape
end
functionelliclick(this, h,e)
this.shapes{end+1} = imellipse(this.imax);
this.newShapeCreated; % add tag, and callback to new shape
end
functionfreeclick(this,h,e)
this.shapes{end+1} = imfreehand(this.imax);
this.newShapeCreated; % add tag, and callback to new shape
end
functionrectclick(this,h,e)
this.shapes{end+1} = imrect(this.imax);
this.newShapeCreated; % add tag, and callback to new shape
end
functiondeleteclick(this,h,e)
        % delete currently selected shape
if ~isempty(this.current) &&this.current> 0
```

```
                n = findobj(this.imax, 'Tag',['imsel_',
num2str(this.current)]);
delete(n);
                % renumbering of this.shapes: (e.g. if 3 deleted:
4=>3, 5=>4,...
fori=this.current+1:numel(this.shapes)
set(this.shapes{i},'Tag',['imsel_', num2str(i-1)]);
end
this.shapes(this.current)=[];
this.current = numel(this.shapes);
this.updateROI;
else
disp('first select a shape to remove');
end
end
functionapplyclick(this, h, e, varargin)
set(this.tl,'String','ROI
applied','Visible','on','BackgroundColor','g');
this.roi = this.mask;
            [this.labels, this.number] = bwlabel(this.mask);
if~(nargin> 3 &&strcmp(varargin{1},'nopreview'))
                % preview window
figure,imshow(label2rgb(this.labels),'InitialMagnification','fit');
title({'This is your labeled ROI', ...
                        ['you have ', num2str(this.number), '
independent region(s)']});
end
notify(this, 'MaskDefined');
end
functionsaveROI(this, h,e)
        % save Mask to File
try
                [this.filename, this.pathname] =
uiputfile('*.mask','Save Mask as',this.filename);
logicmask = this.mask;
save([this.pathname, this.filename],'logicmask','-mat');
set(this.tl,'String',['ROI saved: '
this.filename],'Visible','on','BackgroundColor','g');
```

```
catch
                % aborted
end
end
functionopenROI(this, h,e)
        % load Mask from File
this.newROI; % delete stuff
          [this.filename,this.pathname,~] = uigetfile('*.mask');
try
              b = load([this.pathname,this.filename],'-mat');
if size(b.logicmask)~=size(this.image)
set(this.tl,'String',['Size not matching! '
this.filename],'Visible','on','BackgroundColor','r');
else
this.loadmask = b.logicmask;
this.updateROI;
set(this.tl,'String',['Current: '
this.filename],'Visible','on','BackgroundColor','g');
end
catch
              % aborted
end
end
functionnewROI(this, h,e)
this.mask = zeros(size(this.image));
this.loadmask = zeros(size(this.image));
            % remove all the this.shapes
fori=1:numel(this.shapes)
delete(this.shapes{i});
end
this.current = 1; % defines the currently selected shape - start with
1
this.shapes = {}; % reset shape holder
this.updateROI;
end
        % UI FUNCTIONS ------------------------------------------
------
```

```
functioncreateWindow(this, w, h)
this.guifig=figure('MenuBar','none','Resize','on','Toolbar','none','N
ame','Analyzer - ROI Editor', ...
                'NumberTitle','off','Color','white',
'units','pixels','position',[0 0 this.figwthis.figh],...
                'CloseRequestFcn',@this.closefig, 'visible','off');
            % buttons
buttons = [];
buttons(end+1) =
uicontrol('Parent',this.guifig,'String','Polygon',...
                                        'units','normalized',...
                                        'Position',[0.01 0.8 0.15
0.15], ...

'Callback',@(h,e)this.polyclick(h,e));
buttons(end+1) =
uicontrol('Parent',this.guifig,'String','Ellipse',...
                                        'units','normalized',...
                                        'Position',[0.01 0.65 0.15
0.15],...
'Callback',@(h,e)this.elliclick(h,e));
buttons(end+1) =
uicontrol('Parent',this.guifig,'String','Freehand',...
                                        'units','normalized',...
                                        'Position',[0.01 0.5 0.15
0.15],...
'Callback',@(h,e)this.freeclick(h,e));
buttons(end+1) =
uicontrol('Parent',this.guifig,'String','Rectangle',...
                                        'units','normalized',...
                                        'Position',[0.01 0.35 0.15
0.15],...
'Callback',@(h,e)this.rectclick(h,e));
buttons(end+1) = uicontrol('Parent',this.guifig,'String','Delete',...
                                        'units','normalized',...
                                        'Position',[0.01 0.2 0.15
0.15],...
'Callback',@(h,e)this.deleteclick(h,e));
```

```
buttons(end+1) = uicontrol('Parent',this.guifig,'String','Apply',...
                                        'units','normalized',...
                                        'Position',[0.01 0.05 0.15
0.15],...
'Callback',@(h,e)this.applyclick(h,e));
            % axes
this.imax =
axes('parent',this.guifig,'units','normalized','position',[0.18 0.07
0.4 0.87]);
this.roiax =
axes('parent',this.guifig,'units','normalized','position',[0.59 0.07
0.4 0.87]);
linkaxes([this.imaxthis.roiax]);
            % create toolbar
this.createToolbar(this.guifig);
            % add listeners
set(this.guifig,'WindowButtonDownFcn',@(h,e)this.winpressed(h,e,'down
'));
set(this.guifig,'WindowButtonUpFcn',@(h,e)this.winpressed(h,e,'up'))
;
            % axis titles
uicontrol('tag','txtimax','style','text','string','WorkingArea','unit
s','normalized',...
                        'position',[0.18 0.95 0.4 0.05], ...
                        'BackgroundColor','w');
uicontrol('tag','txtroiax','style','text','string','ROIPreview','unit
s','normalized',...
                        'position',[0.59 0.95 0.4 0.05], ...
        'BackgroundColor','w');
            % file load info
            this.tl =
uicontrol('tag','txtfileinfo','style','text','string','','units','nor
malized',...
                        'position',[0.18 0.01 0.81 0.05], ...
                        'BackgroundColor','g','visible','off');
end
functionresizeWindow(this)
            [h,w]=size(this.image);
```

```
            f = w/h;
this.figw = this.figh*this.hwar*f;
set(this.guifig,'position',[0 0 this.figwthis.figh]);
movegui(this.guifig,'center');
set(this.guifig,'visible','on');
end
functiontb=createToolbar(this, fig)
tb = uitoolbar('parent',fig);
hpt=[];
hpt(end+1) =
uipushtool(tb,'CData',localLoadIconCData('file_new.png'),...
                        'TooltipString','New ROI',...
'ClickedCallback',...
                        @this.newROI);
hpt(end+1) =
uipushtool(tb,'CData',localLoadIconCData('file_open.png'),...
                        'TooltipString','Open ROI',...
'ClickedCallback',...
                        @this.openROI);
hpt(end+1) =
uipushtool(tb,'CData',localLoadIconCData('file_save.png'),...
                        'TooltipString','Save ROI',...
'ClickedCallback',...
                        @this.saveROI);

            %---
hpt(end+1) =
uitoggletool(tb,'CData',localLoadIconCData('tool_zoom_in.png'),...
                        'TooltipString','Zoom In',...
'ClickedCallback',...
'putdowntext(''zoomin'',gcbo)',...
                       'Separator','on');
hpt(end+1) =
uitoggletool(tb,'CData',localLoadIconCData('tool_zoom_out.png'),...
                        'TooltipString','Zoom Out',...
'ClickedCallback',...
'putdowntext(''zoomout'',gcbo)');
```

```
hpt(end+1) =
uitoggletool(tb,'CData',localLoadIconCData('tool_hand.png'),...
                         'TooltipString','Pan',...
'ClickedCallback',...
'putdowntext(''pan'',gcbo)');
end
end  % end private methods
end


% this is copied from matlabsuitoolfactory.m, to load the icons for
the toolbar
functioncdata = localLoadIconCData(filename)
% Loads CData from the icon files (PNG, GIF or MAT) in
toolbox/matlab/icons.
% filename = info.icon;
    % Load cdata from *.gif file
persistent ICONROOT
ifisempty(ICONROOT)
        ICONROOT =
fullfile(matlabroot,'toolbox','matlab','icons',filesep);
end
if length(filename)>3 &&strncmp(filename(end-3:end),'.gif',4)
        [cdata,map] = imread([ICONROOT,filename]);
        % Set all white (1,1,1) colors to be transparent (nan)
ind = map(:,1)+map(:,2)+map(:,3)==3;
map(ind) = NaN;
cdata = ind2rgb(cdata,map);
        % Load cdata from *.png file
elseif length(filename)>3 &&strncmp(filename(end-3:end),'.png',4)
        [cdata map alpha] =
imread([ICONROOT,filename],'Background','none');
        % Converting 16-bit integer colors to MATLAB colorspec
cdata = double(cdata) / 65535.0;
        % Set all transparent pixels to be transparent (nan)
cdata(alpha==0) = NaN;
        % Load cdata from *.mat file
else
```

```
temp = load([ICONROOT,filename],'cdata');
cdata = temp.cdata;
end
end
```

MATLAB Code 4

This code was originally coded by Jonas Reber on 6th May 2011 but modified as per the need of the project. This is for creating the Region of Interest or Mask.

```
function example2
[filename, pathname, filterindex] = uigetfile( ...
{  '*.jpg','JPEG (*.jpg)'; ...
   '*.bmp','Windows Bitmap (*.bmp)'; ...
   '*.fig','Figures (*.fig)'; ...
   '*.*',  'All Files (*.*)'}, ...
   'Choose image(s) to be processed', ...
   'MultiSelect', 'off');
iffilterindex==0, return;
end
filename=cellstr(filename);
myimage = imread(horzcat(pathname,char(filename)));
roiwindow = CROIEditor2(myimage);
addlistener(roiwindow,'MaskDefined',@your_roi_defined_callback)
functionyour_roi_defined_callback(h,e)
            [mask, labels, n] = roiwindow.getROIData;
delete(roiwindow);
end
end
```

MATLAB Code 5

This is for measuring the area of pavement distress in pixels.

```
%%load image
I1= imread('Back.jpg');
%figure
imshow(I1);
title('Background image');
[filename, pathname, filterindex] = uigetfile( ...
{  '*.jpg','JPEG (*.jpg)'; ...
   '*.bmp','Windows Bitmap (*.bmp)'; ...
   '*.fig','Figures (*.fig)'; ...
   '*.*',  'All Files (*.*)'}, ...
   'Choose image(s) to be processed', ...
   'MultiSelect', 'off');
iffilterindex==0, break;end
filename=cellstr(filename);
I2= imread(horzcat(pathname,char(filename)));
%figure
imshow(I2);
title('ROI image');
%% Substract the image
I3= I1 - I2;
%figure
imshow(I3);
title('Substracted Image');
%% Measurements
distress = sum(I3(:));
```